Extension of the Euler–Bernoulli model of piezoelectric laminates to include 3D effects via a mixed approach

Corrado Maurini, Joël Pouget, Francesco Dell'Isola

Extension of the Euler–Bernoulli model of piezoelectric laminates to include 3D effects via a mixed approach

Corrado Maurini [a,b], Joël Pouget [a,*], Francesco dell'Isola [c]

[a] *Laboratoire d'Etudes Mécaniques des Assemblages (FRE 2481), Université de Versailles/Saint-Quentin-en-Yvelines, 45 Avenue des Etats-Unis, 78035 Versailles Cedex, France*

[b] *Dipartimento di Meccanica ed Aeronautica, Università di Roma "La Sapienza", via Eudossiana 18, 00184 Roma, Italy*

[c] *Dipartimento di Ingegneria Strutturale e Geotecnica, Università di Roma "La Sapienza", via Eudossiana 18, 00184 Roma, Italy*

Received 16 June 2005; accepted 14 January 2006
Available online 22 May 2006

Abstract

In this paper a coupled Euler–Bernoulli model of laminated piezoelectric beams is proposed. It is characterized by accounting for the influence of 3D distribution of mechanical stresses and strains through corrected electromechanical constitutive equations. In particular, the hypothesis of vanishing transverse (width direction) normal stress typical of standard beam models is weakened by imposing vanishing stress resultants. This integral condition is enforced by adopting a mixed variational principle and Lagrange multiplier method. Explicit expressions for the beam constitutive coefficients are given and the sandwich and bimorph piezoelectric benders are studied in details. The model is assessed through comparisons with standard models and 3D finite element results, showing an important enhancement of standard beam theories.

Keywords: Beam; Euler–Bernoulli; Piezoelectric; Laminates; Mixed variational formulation; Transverse stress; Capacitance; Sandwich; Bimorph

1. Introduction

After the intensive research efforts dedicated to the field of smart structures in the last 15 years, the use of piezoelectric materials in engineering applications is now widely diffused. In particular, piezoelectric laminated composites are used in the field of active and passive vibration and shape control, in sensors and actuators, in measuring instruments, in medical apparatus, in micro-electromechanical systems [1].

The design of devices including active piezoelectric materials requires, as a preliminary step, an efficient modelling of the *electrical*, *mechanical and coupling* properties of the host structure, the piezoelectric elements and their interactions. For this reason, a great number of research works dealing with structural modelling of piezoelectric composites can be found (see [2,3] for reviews on the subjects). They can be classified in those attempting to solve exact 3D electromechanical problems [4–6], those concentrating on the derivation of plate models [3] and those reducing to the solution of one-dimensional beam problems. In early works actuating [7] and sensing [8] functions of piezoelectric materials have been studied separately. The current trend is toward the formulation of completely coupled models taking into account the two-fold electromechanical coupling and introducing both electric and mechanical degrees of freedom [9–14]. Coupled electromechanical modelling is necessary for several reasons. On one hand it has been shown that if some electrical effects are discarded, significant errors are introduced also in purely mechanical properties [15]. On the other hand, when piezoelectric composites are integrated in truly electromechanical systems, as in passive shunt damping (see e.g. [16–18]), an accurate knowledge of both the electric and mechanical properties of the devices are important in the design process.

* Corresponding author. Tel.: +33 (0)1 39 25 42 09; fax: +33 (0)1 39 25 30 15.
E-mail address: joel.pouget@meca.uvsq.fr (J. Pouget).

0045-7949/$ - see front matter
doi:10.1016/j.compstruc.2006.01.016

A number of works focus on the analysis of two-layer bimorph and three-layer sandwich benders. Simple electromechanical models for their constitutive behavior are given in [19–22], under the standard Euler–Bernoulli hypotheses. More recently, He [5] and Lim and He [6] propose a three-dimensional approach to two-layer bimorphs and three-layer sandwiches. They combine state form formulation of 3D piezoelectricity with asymptotic methods to get an analytical solution for the thickness distribution of the electromechanical fields as a function of the midplane motion. Essentially, they develop an electromechanical plate theory via an asymptotic approach.

A crucial point is to develop models with a good trade-off between accuracy and complexity. Many interesting and rigorous works have been dedicated to increase the model accuracy by introducing additional state variables to describe higher order effects with shareable and layerwise theories (see e.g. [9,23]). However, especially for vibration control applications [17,24,25], the basic induced strain Euler–Bernoulli model presented in [7] and its extensions for including the two-fold electromechanical coupling are still the most popular because of their simplicity.

Some recent papers [26–28] pointed out that available beam models overlook some fundamental phenomena. In particular, the 1D theories are based either on a plane-stress or on a the plane-strain condition where the actual stress and strain states of a layered beam with thickness polarized ceramics are more complex.

The present paper is dedicated to discuss the problems related to 3D effects in beam modelling of piezoelectric laminates and consequently develop a corrected electromechanical Euler–Bernoulli beam model. The weakness of the available theories and the motivations for the present work are illustrated in details in Section 2. The modelling approach we propose is presented in Section 3. It adopts a mixed variational formulation where the standard plane-stress and plane-strain assumptions are replaced by integral constraints on transverse normal stress. In Section 4, the main results are specialized for sandwich and bimorph piezoelectric benders. In particular, handy analytical formula for the corrected bending stiffness, coupling coefficients, and piezoelectric capacitance are provided. Section 5 focuses on the numerical validation of the proposed model by 3D finite element analysis and on comparisons with standard 1D theories for the cases of sandwich and bimorph beams. In this framework, a detailed discussion of the influence of the different hypotheses on the beam constitutive coefficients is carried out. Section 6 is left for conclusions.

2. Problem statement and objectives

In beam modelling of piezoelectric laminates, the hypotheses of uniaxial stress state is usually accepted (see e.g. [7,11,15,19–23,25,29]). In these references, it is assumed that the stress tensor is in the form (see Fig. 1 for the reference orientation)

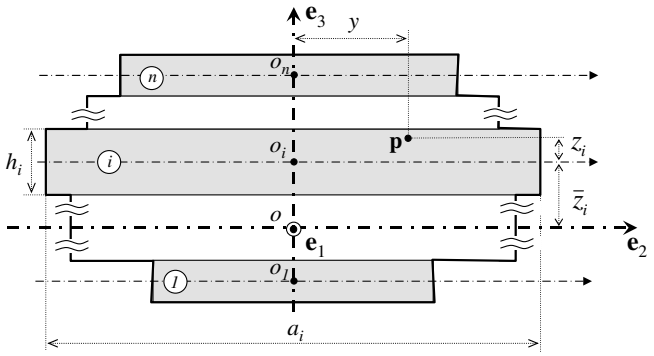

Fig. 1. Generic cross-section of a layered piezoelectric beam having layers with different widths.

$$\mathbf{T} = T_{11}\mathbf{e}_1 \otimes \mathbf{e}_1 \tag{1}$$

and the transverse normal stresses in the beam width direction, T_{22}, are neglected. This hypothesis is accepted also in more accurate 2D approaches which develop either analytical or numerical solutions in the $\mathbf{e}_1$–$\mathbf{e}_3$ plane (i.e. axis-thickness plane) under the plane-stress assumption. The motivations for the neglecting transverse stress are in general similar to those reported explicitly in [12]:

> "Stresses T_{33} and T_{22} can be considered of the order of any loading forces possibly imposed in the x_3- and x_2-directions. Since in our structure we are not considering significant loading forces in these directions, stresses T_{33} and T_{22} can be disregarded, $T_{33} = T_{22} = 0$".

The reasoning above is physically grounded in the theory of single-layer elastic and piezoelectric beams. However, when beams composed of multiple layers are considered, the relations between axial and transverse (along the width) deformations can be different layer by layer and transverse stress can be non-negligible also if transverse loads are not present. In particular, in thickness-polarized piezoelectric layers, the deformations induced by an applied electric potential are isotropic in the $\mathbf{e}_1$–$\mathbf{e}_2$ plane. On the contrary, in elastic layers, an axial extension is usually associated to a transverse shrinking by the classical Poisson effect. When elastic and piezoelectric layers are bonded together, these different behaviors must be reconciled and non-negligible transverse stresses T_{22} arise.

Other authors (see e.g. [11]) assume a plane-strain condition by setting to zero the displacement along the width direction. For layered piezoelectric beams this hypothesis does not correspond to any physical situation and, as shown in the following sections, it introduces several inaccuracies on the estimate of the electromechanical constitutive coefficients.

Beckert and Pfundtner [27] show that the actual stress and strain state of a layered beam with thickness polarized ceramics is typically three-dimensional, being in between the plane-stress and plane-strain conditions. In their paper, they study the strain transfer from piezoelectric to elastic layers by taking into account the effect of the transverse

stress and the influence of the bonding layer. They compare the results obtained for the axial bending induced by an applied potential when assuming three different conditions on the transverse strains and stresses: (i) plane-strain; (ii) plane-stress with a stress distribution of the type (1); (iii) free-bending, which is realized when the layered beam is left free to bend in the transverse direction. Numerical results show that the latter condition is in better agreement with 3D finite element solutions. However, the analysis in [27] is limited to relatively thin piezoelectric layers and it focuses mainly on the strain transfer analysis. In particular, the effect of the transverse deformations and stresses on purely electrical properties of the composite systems, such as the equivalent piezoelectric capacitance, is not considered.

More recently, in the framework of 2D and 3D modelling of piezoelectric bimorphs, Wang [28] discussed the correctness of performing numerical simulation for plates in the cylindrical bending condition, arguing that, due to the in-plane isotropy of the piezoelectric effect, the plane-strain condition cannot be realized in practice. By comparing 3D and 2D numerical results, he showed that the plane-strain hypothesis can lead to significative errors in the estimate of the mechanical displacement induced by an applied electric potential.

In general, not enough attention has been paid to the difference between the plane-stress and plane-strain conditions and the real three-dimensional stress and deformation state. For this reason, the errors between three-dimensional numerical results and estimates from simple beam models were often entirely imputed to neglecting the quadratic contribution of the electric potential [5,6]. A first discussion of this point can be found in [26], where the effect of the transverse bending is investigated by FE numerical simulations.

From the above literature review it seems that an accurate electromechanical Euler–Bernoulli beam model is still missing and that the consequences of neglecting 3D effects on the strain and stress distribution are not fully understood. The present paper is aimed at filling this gap. In the following, an Euler–Bernoulli model where the beam constitutive coefficients correctly account for the influence of transverse stresses and strains is established. To this end, the peculiar geometry of a laminated beam is exploited and ad-hoc hypotheses on the stress distribution are included in the formulation through a mixed approach. This work develops a previous one by the authors [30] by adding an extensive numerical validation and by considering improved assumptions, which describe more faithfully the stress and strain distributions for beams having layers with different widths.

3. Beam model

Under the quasi-electrostatic approximation, the kinematic state of a 3D piezoelectric continuum is determined by the vector field $\mathbf{u}$ and a scalar field φ, representing the mechanical displacement and the electric potential with respect to a grounded reference configuration $\mathscr{B}$. In the linear theory, the corresponding generalized deformations are the mechanical strain tensor $\mathbf{S} = \mathrm{Sym}(\nabla\mathbf{u})$ and the electric field vector $\mathbf{E} = -\nabla\varphi$; the associated generalized forces are the Cauchy stress tensor $\mathbf{T}$ and the electric displacement vector $\mathbf{D}$. By adopting a deductive approach, reduced models of a given structure are derived from the three dimensional description by assuming specific distributions of the state fields. The beam model presented below is derived by a 3D mixed variational formulation for piezoelectricity. The mixed approach let us specify hypotheses both on the kinematic $(\mathbf{u},\varphi)$ and dynamic[1] $(\mathbf{T},\mathbf{D})$ mechanical and electric fields. As shown in the following, a careful choice of the assumed distributions for the mechanical stress and the electric displacement allows for correcting standard models by keeping the same elementary hypotheses on the mechanical displacement and the electric potential.

3.1. 3D mixed variational formulation

Let us consider a three dimensional piezoelectric continuum $\mathscr{B}$ on which the following external actions are applied: body forces $\mathbf{b}$ on the bulk $\mathscr{B}$, surface forces $\mathbf{f}_0$ and surface charges q_0 on the parts $\partial_{\mathbf{f}}\mathscr{B}$ and $\partial_q\mathscr{B}$ of the boundary $\partial\mathscr{B}$, mechanical displacement $\mathbf{u}_0$ and electric potential φ_0 on the parts $\partial_{\mathbf{u}}\mathscr{B}$ and $\partial_\varphi\mathscr{B}$ of $\partial\mathscr{B}$. Let be $\mathscr{V}_{\mathbf{u}}$ and $\mathscr{V}_{\varphi}$ the functional spaces of kinematically compatible mechanical displacement and strain pairs $(\mathbf{u},\mathbf{S})$ and electric potential and electric field pairs $(\varphi,\mathbf{E})$.[2] Moreover let be $\mathscr{V}_{\mathbf{T}}$ and $\mathscr{V}_{\mathbf{D}}$ the spaces of admissible symmetric stress tensors $\mathbf{T}$, and electric displacement vectors $\mathbf{D}$. The solution of the problem of three dimensional piezoelectricity is characterized by rendering stationary the following functional (*Hellinger–Prange–Reissner functional of piezoelectricity*) over the space $\mathscr{V} = \mathscr{V}_{\mathbf{u}} \times \mathscr{V}_{\varphi} \times \mathscr{V}_{\mathbf{T}} \times \mathscr{V}_{\mathbf{D}}$

$$\begin{aligned}\Theta[(\mathbf{u},\mathbf{S}),(\varphi,\mathbf{E}),\mathbf{T},\mathbf{D}] &= \int_{\mathscr{B}} (\mathscr{F}(\mathbf{T},\mathbf{D}) - \mathbf{T}\cdot\mathbf{S} + \mathbf{D}\cdot\mathbf{E} + \mathbf{b}\cdot\mathbf{u})\,\mathrm{d}\mathscr{B} \\ &\quad + \int_{\partial_{\mathbf{f}}\mathscr{B}} \mathbf{f}_0\cdot\mathbf{u}\,\mathrm{d}\mathscr{S} + \int_{\partial_q\mathscr{B}} q_0\varphi\,\mathrm{d}\mathscr{S}. \end{aligned} \tag{2}$$

The scalar valued function $\mathscr{F}(\mathbf{T},\mathbf{D})$ is a piezoelectric internal energy density defined by [31]

$$\mathscr{F}(\mathbf{T},\mathbf{D}) = \frac{1}{2}\mathbf{s}^{\mathrm{D}}\mathbf{T}\cdot\mathbf{T} - \frac{1}{2}\boldsymbol{\beta}^{\mathrm{T}}\mathbf{D}\cdot\mathbf{D} + \mathbf{g}\mathbf{T}\cdot\mathbf{D}, \tag{3}$$

where $\mathbf{s}^{\mathrm{D}}$ is the fourth order elastic compliance tensor for null electric displacement, $\boldsymbol{\beta}^{\mathrm{T}}$ the second order dielectric constants tensor for null mechanical stress, $\mathbf{g}$ the third order piezoelectric coupling tensor.

The equations of 3D linear piezoelectricity are equivalent to the Euler equations of the Hellinger–Prange–Reiss-

[1] Here and henceforth the term *dynamic* is used in its etymological sense (e.g. related to force, power) to indicate the state variables which expend power on the kinematic fields.

[2] $\mathbf{S} = \mathrm{sym}(\nabla\mathbf{u})$ on $\mathscr{B}$ and $\mathbf{u} = \mathbf{u}_0$ on $\partial_{\mathbf{u}}\mathscr{B}$; $\mathbf{E} = -\nabla\varphi$ on $\mathscr{B}$ and $\varphi = \varphi_0$ on $\partial_\varphi\mathscr{B}$.

ner functional (2): the mechanical and electrical balance equations and natural boundary conditions are the Euler equations corresponding to variations of $\mathbf{u}$ and φ; the constitutive equations to variations of $\mathbf{T}$ and $\mathbf{D}$. The essential boundary conditions are included in the definition of the admissible displacement and electric field. The interested reader can found further details about the mixed variational formulation in [32–34].

3.2. Geometry

Consider a multilayered straight-axis piezoelectric beam which is composed by stacking up n rectangular cross-section piezoelectric and elastic layers with width a_i and thickness h_i (see Fig. 1). We denote by $\mathscr{A}$ the beam axis, by $\mathscr{S}$ the beam cross-section, and by $\mathscr{S}_i$ the cross sectional part occupied by the ith layer. Moreover, we regard the rectangular cross-section $\mathscr{S}_i$ as the Cartesian product of a thickness-segment $\mathscr{T}_i$ oriented along the stacking direction and a perpendicular width-segment $\mathscr{W}_i$. The overall beam thickness and width are defined as $\mathscr{T} = \cup_i \mathscr{T}_i$ and $\mathscr{W} = \cup_i \mathscr{W}_i$, respectively. A global Cartesian reference frame $\mathscr{C} = \{o, \mathbf{e}_1, \mathbf{e}_2, \mathbf{e}_3\}$, oriented in such a way that $\mathbf{e}_1$ is aligned along the beam axis, $\mathbf{e}_2$ along the cross sectional width and $\mathbf{e}_3$ along the cross sectional thickness, is fixed once for all and the corresponding coordinates are denoted by (x, y, z). Moreover, n local reference frames $\mathscr{C}_i = \{o_i, \mathbf{e}_1, \mathbf{e}_2, \mathbf{e}_3\}$, with $o_i = o + \bar{z}_i \mathbf{e}_3$, are introduced, and the local coordinates are denoted by (x, y, z_i) where $z_i = z - \bar{z}_i$ and the local origin is chosen so as to satisfy

$$\int_{\mathscr{T}_i} z_i \, \mathrm{d}z = 0.$$

Let be $\mathscr{I} = \{1, \ldots, n\}$ and $\mathscr{I}_e$ and $\mathscr{I}_p$ the subset of $\mathscr{I}$ collecting the indices corresponding to elastic and piezoelectric layers, respectively. In order to account for a beam composed of layers with different dimensions, for each x and y, we define $\mathscr{I}(x, y)$ as the subset of $\mathscr{I}$ collecting only the indices associated to the layers intersected by the z-line of coordinates (x, y). Moreover, we partition also the set $\mathscr{I}(x, y)$ in the set of the indices corresponding to elastic layers, $\mathscr{I}_e(x, y)$, and in the set of indices corresponding to piezoelectric layers, $\mathscr{I}_p(x, y)$.

The following geometric and material properties are assumed: (i) each layer is materially homogeneous and either orthotropic or transversely isotropic with respect to an axis oriented along the stacking direction (in particular the piezoelectric layers are polarized along the thickness); (ii) the upper and lower surfaces of the piezoelectric layers are covered by a conductive layer with negligible mechanical properties, the lateral ones are bared; (iii) the electrodes of the piezoelectric layers are connected in parallel one to each other, and the whole beam is electrically accessible only through two external electric terminals; (iv) the cross-section of the laminate is assumed to be symmetric with respect to the $\mathbf{e}_3$-axis (see Fig. 1). For each piezoelectric layer, we define a constant $\omega_i = \pm 1$ which determines the electric connection scheme between the electrodes of the ith layer and the external terminals ($\omega_i = 1$ in-phase connection, $\omega_i = -1$ counter-phase connection).

Dealing with a *laminated* beam, in addition to the standard beam geometrical hypothesis (i.e. that the ratio $\mathit{length}(\mathscr{A})/\mathit{diameter}(\mathscr{S})$ is high), we assume also that for each lamina both the ratios $\mathit{length}(\mathscr{A})/\mathit{length}(\mathscr{W}_i)$ and $\mathit{length}(\mathscr{W}_i)/\mathit{length}(\mathscr{T}_i)$ are high.

Considering a beam of finite length l, the present analysis will account for the following external actions: (i) a force distribution on the beam bases having a force resultant $\mathbf{F} = \overline{N}\mathbf{e}_1 + \overline{T}\mathbf{e}_3$ and a moment resultant $\mathbf{M} = -\overline{M}\mathbf{e}_2$; (ii) a body force per unit of volume $\mathbf{b}(x, y, z)$ having cross sectional force and moment resultants $\mathbf{b}_R(x) = b_N(x)\mathbf{e}_1 + b_T(x)\mathbf{e}_3$ and $\mathbf{m}_R(x) = -b_M(x)\mathbf{e}_2$, respectively; (iii) either a voltage $\overline{V}$ or a total charge $\overline{Q}$ imposed at the electric terminals of the piezoelectric layers.

3.3. Hypotheses

When deducing structural models from the mixed variational formulation presented above, the system mechanical and electrical equilibrium equations are determined by the hypotheses on the kinematic fields (mechanical displacement and electric potential). On the other hand, the corresponding constitutive prescriptions are influenced by the hypotheses on the dynamic fields (mechanical stress and electric displacement). We fully exploit this property in order to introduce the effect of 3D stresses and strains and of the induced electric potential in a simple Euler–Bernoulli model of laminated piezoelectric beams. In the following, we list the adopted assumptions on the distributions of the electromechanical fields and, successively, we comment about their meaning in the mixed variational setting.

3.3.1. Assumptions on the distribution of the electromechanical fields

Euler–Bernoulli models of piezoelectric beams are usually based on the following hypotheses on the mechanical displacement and electric potential:

(K1) *Mechanical displacement.* Basic equivalent-single-layer Euler–Bernoulli kinematics:

$$\mathbf{u}(x, y, z) = (u(x) - z w'(x))\mathbf{e}_1 + w(x)\mathbf{e}_3, \tag{4}$$

where $u(x)$ and $w(x)$ are the beam axis displacements along $\mathbf{e}_1$ and $\mathbf{e}_3$, respectively.

(K2) *Electric potential.* Layerwise linear distribution of the electric potential, which, when the different layers are electrically interconnected in parallel (either in-phase, $\omega_i = 1$, or in counter-phase, $\omega_i = -1$), is given by the following expression

$$\varphi(x, y, z) = \left(\frac{1}{2} + \omega_i \frac{z_i}{h_i}\right) V, \tag{5}$$

where V is the electric potential difference across the two external electric terminals.

Unfortunately, a model deduced from a standard variational principle with the kinematic hypotheses above will lead to systematic errors in the estimate of the constitutive coefficients of a piezoelectric laminate. The three dimensional distribution of the electromechanical fields will not be correctly simulated, mainly because: (i) the hypothesis (4) on the mechanical displacement implies that the beam cross-sections remain rigid (in [35] the analog problem on plates theory is discussed); (ii) the hypothesis (5) on the electric potential enforces the quadratic part of the electric potential to vanish also in bent piezoelectric layers and neglects the so called "induced electric potential" [10,15,13].

In this paper, we retain the hypotheses (K1) and (K2) on the mechanical and electrical kinematic fields. However, differing from standard modelling approaches, we embed them in the mixed variational setting. In this framework, we assume the following additional conditions on the dynamic fields (e.g. mechanical stress and the electric displacement).

(D1) *Mechanical stress*. A stress tensor composed of axial and transverse normal stresses having constant ($\sigma_{\alpha,i}$) and linear ($\zeta_{\alpha,i}$) contributions through the thickness of each layer

$$\begin{aligned}\mathbf{T}(x,y,z) = {} & (\sigma_{1,i}(x,y) - z_i\zeta_{1,i}(x,y))(\mathbf{e}_1 \otimes \mathbf{e}_1) \\ & + (\sigma_{2,i}(x,y) - z_i\zeta_{2,i}(x,y))(\mathbf{e}_2 \otimes \mathbf{e}_2)\end{aligned} \tag{6}$$

and respecting the following conditions on the through-the-thickness force (n_2) and moment (m_2) resultants of transverse stresses

$$\begin{cases} n_2(x,y) = \displaystyle\sum_{i\in\mathscr{I}(x,y)} \int_{\mathscr{T}_i} \mathbf{T}(x,y,z)\mathbf{e}_2 \cdot \mathbf{e}_2 \,\mathrm{d}z = 0, \\ m_2(x,y) = \displaystyle\sum_{i\in\mathscr{I}(x,y)} \int_{\mathscr{T}_i} -z\mathbf{T}(x,y,z)\mathbf{e}_2 \cdot \mathbf{e}_2 \,\mathrm{d}z = 0. \end{cases} \tag{7}$$

(D2) *Electric displacement*. Layerwise constant distribution along the thickness direction:

$$\mathbf{D}(x,y,z) = D_i(x,y)\mathbf{e}_3, \tag{8}$$

where $D_i(x,y)$ is the function giving the $\mathbf{e}_3$ component of the electric displacement in the ith layer.

3.3.2. Comments

The mixed variational approach and the different kinematic (K1–K2) and dynamic (D1–D2) hypotheses on the electromechanical fields could generate confusion and they deserve some comments and remarks:

- At first sight, the hypothesis (D1) on the transverse stress appears to be not compatible with hypothesis (K1), which assumes rigid cross-sections. Moreover, for bent piezoelectric layers, the hypothesis (D2) of constant electric displacement appears to be not compatible with hypothesis (K2) of linear electric potential. A deeper understanding of the combined effect of the different hypotheses can be get by keeping in mind their role in the mixed variational formulation. In this context, the kinematic hypotheses determine the beam equilibrium equations. On the other hand, the dynamic hypotheses control the field distribution used to estimate the beam constitutive coefficients. Hence, the constitutive coefficients of a model with a poor kinematics (K1 and K2) can account for a more realistic field distribution, which is specified through the hypotheses on the dynamic fields (D1 and D2). This property of the mixed variational formulation is particularly useful when a priori estimates on the dynamic fields are available.
- The two hypotheses on the dynamic fields (D1–D2) allow to get a better agreement with 3D models for two reasons:
  (i) Notwithstanding the elementary Euler–Bernoulli kinematics in hypothesis (K1), the beam constitutive relations will include the influence of cross-sectional deformations through hypotheses on transverse stress (D1). Indeed, the influence of a sectional distension along the thickness will be implicitly taken into account by enforcing null normal stress $T_{33} = \mathbf{T}(x,y,z)\mathbf{e}_3 \cdot \mathbf{e}_3$. The influence of sectional extensional deformations along $\mathbf{e}_2$ will be introduced by constraining the admissible transverse normal stress $T_{22} = \mathbf{T}(x,y,z)\mathbf{e}_2 \cdot \mathbf{e}_2$ with the integral conditions (7). These conditions let the cross-sections free to extend and bend in the transverse direction, respecting the bonding condition between the different layers.
  (ii) The linear distribution of the electric potential assumed in (K2) specifies the electric kinematics only as a function of the potential difference V. However, because of the hypothesis (D2), the beam constitutive equations will account for the through-the-thickness linear contribution to the electric field (quadratic electric potential), which is associated to flexural strains.
- The integral conditions (7) on transverse stresses will be enforced in the mixed variational formulation through the Lagrange multiplier method. The physical interpretation of the corresponding Lagrange multipliers show that the conditions (7) introduce the effect of non-uniform transverse bending and extension of the beam cross-sections. Details about this point are given in Subsection 3.4.
- The mixed variational approach with the hypotheses (4)–(8) introduces in a simple way the effects of cross-sectional deformations and the quadratic contributions to the electric potential in the beam constitutive equations. However, the present model is not equivalent to a model where these effects are introduced directly through an enriched kinematics in the context of a

standard variational formulation. In particular, it neglects the shear-like effects which are present when two adjacent cross-sections experience different transverse deformations. Moreover, it ignores that, when the quadratic contribution of the electric potential is not constant inside a piezoelectric layer, the electric field and electric displacement become more complex than those in (5) and (8) since components in the $\mathbf{e}_1$–$\mathbf{e}_2$ plane appear.

- In hypothesis (6) the shear terms of the stress tensor are set to zero. This assumption, although very far from being verified in a 3D model, does not imply any error in the resulting Euler–Bernoulli beam model, because: (i) the displacement field (4) automatically accounts for an infinite shear stiffness (the cross sections remain orthogonal to the beam axis); (ii) in orthotropic materials the assumptions on the shear stresses have no influence on the constitutive relations between normal stresses and strains, since they are constitutively uncoupled.
- The hypothesis (7) substitutes an averaged version used in a previous paper by the authors [30], where the integral was taken across the entire cross-section instead that along each thickness segment. The present hypothesis is more accurate in the case of beams composed by layers with different widths. It imposes the integral condition on the transverse stress at each z-line instead that, in an averaged sense, on each cross-section. Hence, it allows the beam to have non-uniform transverse stress along the width and, consequently, to experience non-uniform transverse deformations.

The present model, and in particular hypothesis (D1), relies on the assumption that the beam is composed of a stack of laminae. In other words, the proposed model is applicable to beam having the cross-sectional geometry in Fig. 1, where the thickness h_i, the width a_i, and the length l_i of each layer are such that $l_i \gg a_i \gg h_i$. As a rule of thumb, the results presented in this paper are accurate if $l_i \geqslant \alpha a_i$ and $a_i \geqslant \alpha h_i$ with $\alpha \simeq 5$.

3.4. 1D mixed variational formulation with integral conditions on transverse stress

In a beam model accounting for the hypotheses (4)–(8), the distributions of the three dimensional state fields $(\mathbf{u}, \varphi, \mathbf{T}, \mathbf{D})$ is uniquely determined by the fields

$$\{u(x), w(x), V, \sigma_{\alpha,i}(x,y), \zeta_{\alpha,i}(x,y), D_i(x,y)\},$$

where the electric voltage V has been assumed to be constant because the surfaces of the transducers are equipotential. Here and henceforth, the mute indices α and i are intended to vary from 1 to 2 and from 1 to n, respectively.

By introducing the hypotheses (4)–(8) into the functional (2), a beam mixed functional

$$\Theta_{\text{beam}}[u, w, V, \sigma_{\alpha,i}, \zeta_{\alpha,i}, D_i]$$

is deduced. It is defined over the functional space of admissible beam state fields $(u, w, V, \sigma_{\alpha,i}, \zeta_{\alpha,i}, D_i)$. This space will be denoted by $\mathscr{W}$.

The integral conditions (7) on transverse stresses can be conveniently introduced in the variational formulation by the Lagrange multiplier methods. To this end the following extended functional is defined:

$$\begin{aligned}\Theta^{\Lambda}_{\text{beam}}[u, w, \sigma_{\alpha,i}, \zeta_{\alpha,i}, D_i, V, \lambda, \mu] &= \Theta_{\text{beam}}[u, w, \sigma_{\alpha,i}, \zeta_{\alpha,i}, D_i, V] - \int_{\mathscr{A}\times\mathscr{W}} \lambda(x,y) n_y(x,y)\,\mathrm{d}x\,\mathrm{d}y \\ &\quad - \int_{\mathscr{A}\times\mathscr{W}} \mu(x,y) m_y(x,y)\,\mathrm{d}x\,\mathrm{d}y. \end{aligned} \tag{9}$$

The Lagrange multipliers fields $\lambda(x,y)$ and $\mu(x,y)$ enforce, along each z-line identified by the coordinates (x,y), the conditions (7) of vanishing transverse force and moment resultants. The corresponding variational formulation consists of looking for those beam state fields in $\mathscr{W}$ and those admissible Lagrange multipliers (λ, μ) rendering stationary the functional $\Theta^{\Lambda}_{\text{beam}}$.

Remark 1. The Lagrange multipliers λ and μ are the transverse analogs of the axial deformations u' and w''. They can be interpreted as constant (λ) and linear (μ) contributions to the $\mathbf{e}_2$-normal strain throughout the z-line identified by coordinates (x,y). Note that they explicitly depend not only on x but also on y.

3.5. Derivation of the beam model

3.5.1. Definitions

For a generic z-line of coordinates (x,y), let us introduce the following force and moment stress resultants along the thickness $\mathscr{T}_i$ of the generic ith layer intersected by that line

$$n_{\alpha,i}(x,y) = \int_{\mathscr{T}_i} \sigma_{\alpha,i}(x,y)\,\mathrm{d}z = h_i \sigma_{\alpha,i}(x,y),$$
$$m_{\alpha,i}(x,y) = \int_{\mathscr{T}_i} z_i^2 \zeta_{\alpha,i}(x,y)\,\mathrm{d}z = \frac{h_i^3}{12}\zeta_{\alpha,i}(x,y)$$

and the force and moment resultants along the whole beam thickness

$$n_\alpha(x,y) = \sum_{i\in\mathscr{I}(x,y)} n_{\alpha,i}(x,y),$$
$$m_\alpha(x,y) = \sum_{i\in\mathscr{I}(x,y)} m_{\alpha,i}(x,y) - \sum_{i\in\mathscr{I}(x,y)} \bar{z}_i n_{\alpha,i}(x,y).$$

Moreover, let us define the charge per unit surface on the electrodes as

$$\chi(x,y) = -\sum_{i\in\mathscr{I}_p(x,y)} \omega_i D_i(x).$$

The total force and moment resultants of axial stress and the charge per unit line on the entire beam cross section at the axial point x can be written as

$$N_1(x) = \int_{\mathscr{W}} n_1(x,y)\,\mathrm{d}y, \tag{10a}$$

$$M_1(x) = \int_{\mathscr{W}} (m_1(x,y) - \bar{z}_i n_1(x,y))\,\mathrm{d}y, \tag{10b}$$

$$q(x) = \int_{\mathscr{W}} \chi(x,y)\,\mathrm{d}y = -\sum_{i\in\mathscr{I}_p(x,y)} \omega_i D_i(x) a_i. \tag{10c}$$

Moreover, let us list the fields associated to the axial and transverse deformations, transverse force and moment resultants as follows

$$\mathbf{d}_1(x) = \begin{bmatrix} u'(x) \\ w''(x) \end{bmatrix}, \quad \mathbf{d}_2(x,y) = \begin{bmatrix} \lambda(x,y) \\ \mu(x,y) \end{bmatrix}, \tag{11}$$

$$\mathbf{r}_\alpha(x,y) = \begin{bmatrix} n_\alpha(x,y) \\ m_\alpha(x,y) \end{bmatrix}, \quad \mathbf{R}_1(x) = \begin{bmatrix} N_1(x) \\ M_1(x) \end{bmatrix}. \tag{12}$$

3.5.2. Euler–Lagrange equations of the mixed functional

By imposing that the mixed functional Θ^A_{beam} is stationary for all the admissible beam state fields $(u, w, V, \sigma_{\alpha,i}, \zeta_{\alpha,i}, D_i)$ and for all the admissible Lagrange multiplier fields (λ, μ), we obtain the following Euler–Lagrange equations of the variational problem.

(a) The beam balance equations and natural boundary conditions (from variations with respect to u, w, and V):

$$\begin{cases} b_N(x) + N_1'(x) = 0, \\ b_M'(x) - b_T(x) + M_1''(x) = 0, \\ \displaystyle\int_{\mathscr{A}} q(x)\,\mathrm{d}x + \overline{Q} = 0 \end{cases} \tag{13}$$

and

$$[(N_1 - \overline{N})\delta u]_{\partial\mathscr{A}} = 0, \tag{14a}$$

$$[(M_1 - \overline{M})\delta w' + (\overline{T} + M_1' + b_M)\delta w]_{\partial\mathscr{A}} = 0. \tag{14b}$$

where in the latter variational expressions for the boundary conditions δu, δw and $\delta w'$ denote arbitrary admissible variations of u, w and w'.

(b) The conditions (7) on transverse stresses (from variations with respect to λ and μ), which can be rewritten in the form:

$$\mathbf{r}_2(x,y) = \mathbf{0}. \tag{15}$$

(c) The local (layer by layer) constitutive equations in terms of axial deformations, transverse deformations and electric voltage (from variations with respect to $\sigma_i^{(\alpha)}$, $\zeta_i^{(\alpha)}$, and D_i):

$$\text{piezoelectric layers } i\in\mathscr{I}_p \begin{cases} \sigma_{\alpha,i} = \tilde{c}^{\mathrm{E}}_{\alpha\beta}\varepsilon_{\beta,i} + \tilde{e}_{3\alpha}\mathsf{E}_{3,i}, \\ \zeta_{\alpha,i} = \tilde{c}^{\mathrm{D}}_{\alpha\beta}\kappa_{\beta,i}, \\ \mathsf{D}_{3,i} = -\tilde{e}_{3\beta}\varepsilon_{\beta,i} + \tilde{\epsilon}^S_{33}\mathsf{E}_{3,i} \end{cases} \tag{16a}$$

$$\text{elastic layers } i\in\mathscr{I}_e \begin{cases} \sigma_{\alpha,i} = \tilde{c}_{\alpha\beta}\varepsilon_{\beta,i}, \\ \zeta_{\beta,i} = \tilde{c}_{\alpha\beta}\kappa_{\beta,i}. \end{cases} \tag{16b}$$

The definitions of the constitutive coefficients appearing above are given in Table 1 and

Table 1
Plane-strain constitutive coefficients in the S-E form for the piezoelectric and elastic layers as a function of the 3D material data given in the T-D form

Elastic layers	
$\tilde{c}_{11} = \dfrac{1}{s_{11}}\dfrac{1}{1-\nu^2}$	$\tilde{c}_{12} = \nu\tilde{c}_{11}$
$\nu = -s_{12}/s_{11}$	
Piezoelectric layers	
$\tilde{c}^{\mathrm{E}}_{11} = \dfrac{1}{s^{\mathrm{E}}_{11}}\dfrac{1}{1-(\nu^{\mathrm{E}})^2}$	$\tilde{c}^{\mathrm{D}}_{11} = \tilde{c}^{\mathrm{E}}_{11}(1+\gamma^2)$
$\tilde{c}^{\mathrm{E}}_{12} = \nu^{\mathrm{E}}\tilde{c}^{\mathrm{E}}_{11}$	$\tilde{c}^{\mathrm{D}}_{12} = \tilde{c}^{\mathrm{E}}_{12}(1+\gamma^2/\nu^{\mathrm{E}})$
$\tilde{e}_{31} = \dfrac{d_{31}}{s^{\mathrm{E}}_{11}(1-\nu^{\mathrm{E}})}$	$\tilde{\epsilon}^S_{33} = \dfrac{1}{\beta^{\mathrm{T}}_{33}}\left(1 - \dfrac{2\beta^{\mathrm{T}}_{33}d^2_{31}}{s^{\mathrm{E}}_{11}(1-\nu^{\mathrm{E}})}\right)$
$\nu^{\mathrm{E}} = -s^{\mathrm{E}}_{12}/s^{\mathrm{E}}_{11}$	$\gamma = \sqrt{\dfrac{d^2_{31}\beta^{\mathrm{T}}_{33}}{s^{\mathrm{E}}_{11}}\dfrac{(1+\nu^{\mathrm{E}})}{(1-\nu^{\mathrm{E}}) - 2\dfrac{d^2_{31}\beta^{\mathrm{T}}_{33}}{s^{\mathrm{E}}_{11}}}}$

Standard Voigt notation for piezoelectric materials is adopted. The constitutive constants $s^{\mathrm{E}}_{11} = 1/Y^{\mathrm{E}}$, $s^{\mathrm{E}}_{12} = -\nu^{\mathrm{E}}/Y^{\mathrm{E}}$, d_{31} and β^{T}_{33} refer to the piezoelectric ceramic and are those usually provided in the datasheets (see e.g. www.piezo.com); $s_{11} = 1/Y$ and $s_{12} = -\nu/Y$ refer to elastic material; $(Y^{\mathrm{E}}, \nu^{\mathrm{E}})$ and (Y, ν) are the in-plane Young and Poisson modulus for the piezoelectric material (at constant electric field) and for the elastic material, respectively.

$$\varepsilon_{1,i} = u' - \bar{z}_i w'', \quad \kappa_{1,i} = w'',$$
$$\varepsilon_{2,i} = \lambda - \bar{z}_i\mu, \quad \kappa_{2,i} = \mu,$$
$$\mathsf{E}_{3,i} = -(\omega_i/h_i)V$$

are the constant and linear contributions to the mechanical axial $(\varepsilon_{1,i}, \kappa_{1,i})$ and transverse $(\varepsilon_{2,i}, \kappa_{2,i})$ deformations through the ith layer, while $\mathsf{E}_{3,i} = -(\omega_i/h_i)V$ is the constant part of the $\mathbf{e}_3$-component of the electric field.

Remark 2. In the adopted mixed variational formulation the hypotheses on the kinematic fields determine the form of the mechanical equilibrium equations, while the constitutive equations are influenced by the hypotheses on the dynamic fields. Because of the assumed kinematics, the mechanical equilibrium equations are those of a standard Euler–Bernoulli beam, the electric one is the Kirchhoff's law at the external electric terminals.

Remark 3. The coefficients appearing in the local constitutive Eq. (16a) show that in piezoelectric layers the constant contributions to the mechanical deformations $(\varepsilon_{1,i}, \varepsilon_{2,i})$ are associated to the mechanical stiffnesses at constant electric field $(\tilde{c}^{\mathrm{E}}_{\alpha\beta})$, while the linear contributions $(\kappa_{1,i}, \kappa_{2,i})$ are associated to the stiffnesses at constant electric displacement $(\tilde{c}^{\mathrm{D}}_{\alpha\beta})$. This is due to the hypothesis (8) of constant electric displacement, which allows for including the influence of the induced electric potential in the mechanical stiffness [15].

3.5.3. Calculation of effective beam constitutive equations

By introducing the constitutive Eq. (16) into the definitions (12) of the through-the-thickness stress resultants

and into the expression for the electric charge per unit surface χ, we find

$$\mathbf{r}_1(x,y) = \tilde{\mathbf{k}}_{11}(x,y)\mathbf{d}_1(x) + \tilde{\mathbf{k}}_{12}(x,y)\mathbf{d}_2(x,y) - \tilde{\mathbf{e}}^t_{\chi d}(x,y)V, \quad (17a)$$

$$\mathbf{r}_2(x,y) = \tilde{\mathbf{k}}_{12}(x,y)\mathbf{d}_1(x) + \tilde{\mathbf{k}}_{11}(x,y)\mathbf{d}_2(x,y) - \tilde{\mathbf{e}}^t_{\chi d}(x,y)V, \quad (17b)$$

$$\chi(x,y) = \tilde{\mathbf{e}}_{\chi d}(x,y)(\mathbf{d}_1(x) + \mathbf{d}_2(x,y)) + \tilde{\varepsilon}_{\chi V}(x,y)V, \quad (17c)$$

where the stiffness matrices $\tilde{\mathbf{k}}_{11}(x,y)$ and $\tilde{\mathbf{k}}_{12}(x,y)$, the coupling vector $\tilde{\mathbf{e}}_{\chi d}(x,y)$, and the capacitance per unit surface $\tilde{\varepsilon}_{\chi V}(x,y)$ are given by

$$\tilde{\mathbf{k}}_{11}(x,y) = \begin{bmatrix} [\tilde{\mathbf{k}}_{11}(x,y)]_{11} & [\tilde{\mathbf{k}}_{11}(x,y)]_{12} \\ [\tilde{\mathbf{k}}_{11}(x,y)]_{12} & [\tilde{\mathbf{k}}_{11}(x,y)]_{22} \end{bmatrix}, \quad (18a)$$

$$\tilde{\mathbf{k}}_{12}(x,y) = \begin{bmatrix} [\tilde{\mathbf{k}}_{12}(x,y)]_{11} & [\tilde{\mathbf{k}}_{12}(x,y)]_{12} \\ [\tilde{\mathbf{k}}_{12}(x,y)]_{12} & [\tilde{\mathbf{k}}_{12}(x,y)]_{22} \end{bmatrix}, \quad (18b)$$

$$\tilde{\mathbf{e}}_{\chi d}(x,y) = \begin{bmatrix} \sum_{i\in\mathscr{I}_p(x,y)} \omega_i \tilde{e}_{31} & \sum_{i\in\mathscr{I}_p(x,y)} \omega_i \tilde{e}_{31}\bar{z}_i \end{bmatrix}, \quad (18c)$$

$$\tilde{\varepsilon}_{\chi V}(x,y) = \sum_{i\in\mathscr{I}_p(x,y)} \frac{\tilde{\varepsilon}^S_{33}}{h_i}, \quad (18d)$$

with

$$[\tilde{\mathbf{k}}_{\alpha\beta}(x,y)]_{11} = \sum_{i\in\mathscr{I}_p(x,y)} h_i \tilde{c}^{\mathrm{E}}_{\alpha\beta} + \sum_{i\in\mathscr{I}_e(x,y)} h_i \tilde{c}_{\alpha\beta},$$

$$[\tilde{\mathbf{k}}_{\alpha\beta}(x,y)]_{12} = \sum_{i\in\mathscr{I}_p(x,y)} h_i \bar{z}_i \tilde{c}^{\mathrm{E}}_{\alpha\beta} + \sum_{i\in\mathscr{I}_e(x,y)} h_i \bar{z}_i \tilde{c}_{\alpha\beta},$$

$$[\tilde{\mathbf{k}}_{\alpha\beta}(x,y)]_{22} = \sum_{i\in\mathscr{I}_p(x,y)} \left(h_i \bar{z}_i^2 \tilde{c}^{\mathrm{E}}_{\alpha\beta} + \frac{1}{12} h_i^3 \tilde{c}^{\mathrm{D}}_{\alpha\beta} \right) + \sum_{i\in\mathscr{I}_e(x,y)} \tilde{c}_{\alpha\beta} \left(h_i \bar{z}_i^2 + \frac{1}{12} h_i^3 \right).$$

By enforcing the conditions on transverse stress resultants (15), the constitutive Eq. (17b) for the transverse stress resultants can be solved for $\mathbf{d}_2(x,y)$, giving the generalized transverse deformations as a function of the axial ones and the electric voltage

$$\mathbf{d}_2(x,y) = -\tilde{\mathbf{k}}_{11}^{-1}(x,y)\tilde{\mathbf{k}}_{12}(x,y)\mathbf{d}_1(x) + \tilde{\mathbf{k}}_{11}^{-1}(x,y)\tilde{\mathbf{e}}^t_{\chi d}(x,y)V. \quad (19)$$

The substitution of this expression into the constitutive laws (17) for $\mathbf{r}_1$ and χ gives the following reduced constitutive equations, where only the axial deformations $\mathbf{d}_1(x)$ and the electric voltage V appear:

$$\begin{aligned} \mathbf{r}_1(x,y) &= \mathbf{k}_{11}(x,y)\mathbf{d}_1(x) - \mathbf{e}^t_{\chi d}(x,y)V, \\ \chi(x,y) &= \mathbf{e}_{\chi d}(x,y)\mathbf{d}_1(x) + \varepsilon_{\chi V}(x,y)V, \end{aligned} \quad (20)$$

with

$$\begin{aligned} \mathbf{k}_{11}(x,y) &= \tilde{\mathbf{k}}_{11}(x,y) - \tilde{\mathbf{k}}_{12}(x,y)\tilde{\mathbf{k}}_{11}^{-1}(x,y)\tilde{\mathbf{k}}_{12}(x,y), \\ \mathbf{e}_{\chi d}(x,y) &= \tilde{\mathbf{e}}_{\chi d}(x,y) - \tilde{\mathbf{e}}_{\chi d}(x,y)\tilde{\mathbf{k}}_{11}^{-1}(x,y)\tilde{\mathbf{k}}_{12}(x,y), \\ \varepsilon_{\chi V}(x,y) &= \tilde{\varepsilon}_{\chi V}(x,y) + \tilde{\mathbf{e}}_{\chi d}(x,y)\tilde{\mathbf{k}}_{11}^{-1}(x,y)\tilde{\mathbf{e}}^t_{\chi d}(x,y). \end{aligned} \quad (21)$$

Finally, the integration over the cross-sectional width gives the effective constitutive equations for the cross-sectional axial force and moment resultants (N_1, M_1) and the charge per unit line q

$$\begin{aligned} \mathbf{R}_1(x) &= \mathbf{K}(x)\mathbf{d}_1(x) - \mathbf{e}^t_{qd}(x)V, \\ q(x) &= \mathbf{e}_{qd}(x)\mathbf{d}_1(x) + \varepsilon_{qV}(x)V, \end{aligned} \quad (22)$$

where

$$\begin{aligned} \mathbf{K}(x) &= \int_{\mathscr{W}} \mathbf{k}_{11}(x,y)\,\mathrm{d}y, \\ \mathbf{e}_{qd}(x) &= \int_{\mathscr{W}} \mathbf{e}_{\chi d}(x,y)\,\mathrm{d}y, \\ \varepsilon_{qV}(x) &= \int_{\mathscr{W}} \varepsilon_{\chi V}(x,y)\,\mathrm{d}y. \end{aligned} \quad (23)$$

3.6. Beam equations in the final form

The governing equations of the model derived above are in the same form of those of a standard electromechanical Euler–Bernoulli model for piezoelectric beams. They are given by

- The mechanical and electrical equilibrium equation (13). The mechanical natural boundary conditions are found from (14) once the admissible axial and transverse displacement fields, $u(x)$ and $w(x)$, are chosen.
- The beam constitutive equation (22), where the axial force resultant $N_1(x)$, the moment resultant $M_1(x)$ and the electric charge per unit line $q(x)$, are expressed as a function of the axis elongation $u'(x)$, the axis curvature $w''(x)$, and the electric potential difference V. Eq. (22) can be rewritten in an explicit form as follows:

$$\begin{bmatrix} N_1 \\ M_1 \\ q \end{bmatrix} = \begin{bmatrix} k_{Nu} & k_{Nw} & e_{NV} \\ k_{Nw} & k_{Mw} & -e_{MV} \\ -e_{NV} & e_{MV} & \varepsilon_{qV} \end{bmatrix} \begin{bmatrix} u' \\ w'' \\ V \end{bmatrix}, \quad (24)$$

  where the association between the appearing constitutive coefficients and the entries of matrices $\mathbf{K}(x)$ and $\mathbf{e}_{qd}(x)$, defined by (23), is immediate.

The present model differs from standard ones for giving more accurate estimates of the constitutive coefficients appearing in Eq. (24). This point is fully discussed in the next sections, where piezoelectric sandwich and bimorph beams in bending are analyzed in details. For these cases, explicit analytical expressions for the electromechanical constitutive coefficients are given in Section 4. Numerical comparisons with standard models and 3D finite element results are discussed in Section 5. For a generic piezoelectric laminate as in Fig. 1, the constitutive coefficients appearing in Eq. (24) are calculated by Eqs. (23) and (21), considering the definitions given in Eq. (18) and Table 1.

4. Piezoelectric sandwich beam

In this section, we consider the particular layer arrangement shown in Fig. 2, where two identical piezoelectric

layers, polarized along the same direction are bonded on a central elastic layer and are electrically interconnected in parallel and counter-phase. A beam with this layers configuration is called piezoelectric sandwich. It is conceived for coupling the voltage and the charge at the electric terminals to the beam bending, without introducing central axis extension. For this configuration, we provide analytical expressions of the relevant beam constitutive parameters appearing in (24). The case of beams having layers of different widths (see Fig. 2) is considered explicitly. For sandwich beam with thin piezoelectric layers, simplified formulas are derived, while the interesting case of a two-layer bimorph bender is obtained by letting vanish the thickness of the central elastic layer. For comparisons purposes, we report also the expressions of the constitutive coefficients obtained by standard approaches which neglect 3D effects. Namely, we consider the model assuming null transverse deformations (ND), the model assuming null transverse stresses (NS), and the model assuming null transverse stresses and neglecting the influence of the induced potential (NS1).

4.1. Proposed model

4.1.1. Complete expressions

For a piezoelectric sandwich beam, because of the material and geometric symmetry, beam extension and bending are decoupled and the stiffness matrices $\tilde{\mathbf{k}}_{11}$ and $\tilde{\mathbf{k}}_{12}$ defined in Eqs. (18) are diagonal. Moreover, due to the electric interconnection of the two piezoelectric layers, the first term of the coupling vector $\tilde{\mathbf{e}}_{\chi d}$ is null, and an imposed electric potential V induces only a bending moment with a vanishing force resultant. Hence, the constitutive Eq. (24) for the bending moment M_1 and the electric charge per unit line q, being uncoupled from the extensional problem, assume the simplified form

$$\begin{bmatrix} M_1 \\ q \end{bmatrix} = \begin{bmatrix} k_{Mw} & -e_{MV} \\ e_{MV} & \varepsilon_{qV} \end{bmatrix} \begin{bmatrix} w'' \\ V \end{bmatrix}. \tag{25}$$

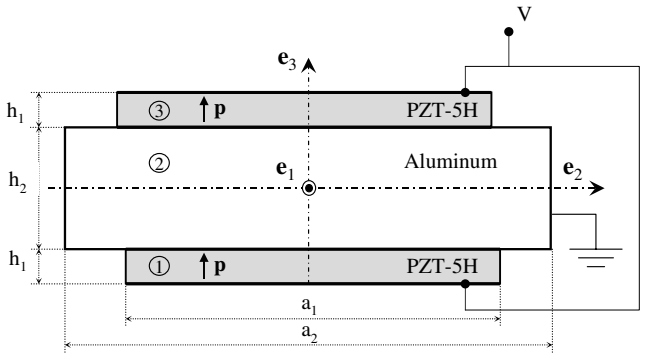

Fig. 2. Cross-section of a piezoelectric sandwich beam with piezoelectric layers connected in parallel and in counter-phase. In this geometrically symmetrical configuration, the electric potential difference and charge are coupled to pure beam bending. A two-layer bending bimorph is obtained when $h_2 \to 0$. The polarization direction of the piezoelectric transducers is denoted by an arrow and the letter "p".

Moreover, since stiffness matrices are diagonal, the calculation implied by Eqs. (21) and (23) can be easily carried out explicitly. The following expressions for the constitutive coefficients in Eq. (25) are found

$$k_{Mw} = a_1 K_{11}\left(1 - \frac{K_{12}^2}{K_{11}^2}\right) + (a_2 - a_1)\frac{1}{12}h_2^3\tilde{c}_{11}(1-\nu^2), \tag{26a}$$

$$e_{MV} = a_1\tilde{e}_{31}(h_1 + h_2)\left(1 - \frac{K_{12}}{K_{11}}\right), \tag{26b}$$

$$\varepsilon_{qV} = \frac{2a_1\tilde{e}_{33}^S}{h_1} + \frac{a_1(\tilde{e}_{31}(h_1+h_2))^2}{K_{11}}, \tag{26c}$$

where the stiffness parameters K_{11}, K_{12} are defined by (see also Table 1):

$$K_{\alpha\beta} = \frac{\tilde{c}_{\alpha\beta}^{\mathrm{E}} h_1^3}{12}\left(6\left(1 + \frac{h_2}{h_1}\right)^2 + 2\frac{\tilde{c}_{\alpha\beta}^{\mathrm{D}}}{\tilde{c}_{\alpha\beta}^{\mathrm{E}}} + \frac{\tilde{c}_{\alpha\beta}}{\tilde{c}_{\alpha\beta}^{\mathrm{E}}}\frac{h_2^3}{h_1^3}\right).$$

Remark 4. In the stiffness parameters $K_{\alpha\beta}$ we can distinguish between three contributions: the first one, proportional to $\tilde{c}_{\alpha\beta}^{\mathrm{E}}$, is associated to the flexural stiffness due to piezoelectric layer extension, the second one, proportional to $\tilde{c}_{\alpha\beta}^{\mathrm{D}}$, is due to piezoelectric layers bending, and the third one, proportional to $\tilde{c}_{\alpha\beta}$, to elastic layer bending.

Remark 5. The electromechanical constitutive coefficients are equal to those of a piezoelectric sandwich beam having the width of the piezoelectric layers, except for the mechanical stiffness (26a). The second term in the right hand side of Eq. (26a) is the additional contribution due to the purely elastic parts of the beam cross-section.

Remark 6. The numerical evaluation of the beam constitutive constants (26) requires only four piezoelectric material coefficients (see Table 1): the piezoelectric in-plane Young's modulus Y^{E} and Poisson's coefficient ν^{E} at constant electric field, the coupling coefficient d_{31}, and the electric constant β_{33}^{T}.

4.1.2. Approximation for thin piezoelectric layers

When the piezoelectric layers are thin with respect to the central elastic one, the constitutive coefficients (26) can be approximated by their first order Taylor expansions in the small parameter

$$\tau = h_1/h_2$$

and the following simplified expressions are found:[3]

[3] Since the piezoelectric capacitance ε_{qV} is singular for $\tau = 0$, its approximation has been found by expanding up to the first order $\varepsilon_{qV}{}^{*}h_1$, the piezoelectric capacitance per unit thickness.

$$k_{Mw}^{(\tau)} = \tilde{c}_{11}(1-\nu)\frac{a_2 h_2^3}{12} + \tau\frac{\tilde{c}_{11}^{\mathrm{E}} h_2^3 a_1}{2}(1+\nu^2-2\nu\nu^{\mathrm{E}}), \tag{27a}$$

$$e_{MV}^{(\tau)} = a_1\tilde{e}_{31}h_2(1-\nu) + \tau a_1\tilde{e}_{31}h_2\left(1-\nu+6(\nu-\nu^{\mathrm{E}})\frac{\tilde{c}_{11}^{\mathrm{E}}}{\tilde{c}_{11}}\right), \tag{27b}$$

$$\varepsilon_{qV}^{(\tau)} = \frac{2a_1\tilde{\varepsilon}_{33}^{S}}{\tau h_2}\left(1+6\gamma^2\frac{\tilde{c}_{11}^{\mathrm{E}}}{\tilde{c}_{11}}\tau\right). \tag{27c}$$

In the linear approximations above, the contribution to the mechanical stiffness due to the bending of the piezoelectric layers is not present and only their membranal behavior is taken into account. Indeed, the bending stiffness becomes independent of the mechanical compliances at constant electric displacement $\tilde{c}_{11}^{\mathrm{D}}$ and $\tilde{c}_{12}^{\mathrm{D}}$. This result proves that the influence of the induced electric potential is negligible for thin piezoelectric layers. On the other hand, the effect of transverse interactions between piezoelectric and elastic layers is present also in this case, as revealed by the dependence of $k_{Mw}^{(\tau)}$ and $e_{MV}^{(\tau)}$ on the Poisson ratios.

4.1.3. Two-layer bimorph

The constitutive coefficients for the bimorph bender constituted by two piezoelectric layers connected in parallel and in counter phase are obtained from expressions (26) by letting the thickness of the elastic layer (h_2) go to zero:

$$k_{Mw}^{(b)} = \frac{4(2+\gamma^2+2\nu^{\mathrm{E}})}{(4+\gamma^2)(1+\nu^{\mathrm{E}})}\frac{a_1 h_1^3 Y^{\mathrm{E}}}{3}, \tag{28a}$$

$$e_{MV}^{(b)} = \frac{4}{4+\gamma^2}a_1 d_{31} Y^{\mathrm{E}} h_1, \tag{28b}$$

$$\varepsilon_{qV}^{(b)} = \frac{2a_1}{h_1\beta_{33}^{\mathrm{T}}}\left(1-d_{31}^2 Y^{\mathrm{E}}\beta_{33}^{\mathrm{T}}\frac{5+2\gamma^2-3\nu^{\mathrm{E}}}{(4+\gamma^2)(1-\nu^{\mathrm{E}})}\right). \tag{28c}$$

4.2. Standard models

4.2.1. Null transverse stress (NS) models

Many authors assume an uniaxial stress-state in the form (1) by replacing the integral constraints (7) on the transverse stress by the hypothesis of pointwise vanishing transverse stress. Under these conditions, the coefficients of the constitutive equation (25) for the piezoelectric sandwich beam in Fig. 2 are found to be (see [30] for the detailed derivation):

$$k_{Mw}^{(\mathrm{NS})} = Y^{\mathrm{E}}(1+\gamma^2)\frac{a_1 h_1^3}{6} + Y^{\mathrm{E}}\frac{a_1 h_1 (h_1+h_2)^2}{2} + Y\frac{a_2 h_2^3}{12}, \tag{29a}$$

$$e_{MV}^{(\mathrm{NS})} = -d_{31}Y^{\mathrm{E}}a_1(h_1+h_2), \tag{29b}$$

$$\varepsilon_{qV}^{(\mathrm{NS})} = \frac{2a_1}{h_1}\frac{1}{\beta_{33}^{\mathrm{T}}}(1-d_{31}^2 Y^{\mathrm{E}}\beta_{33}^{\mathrm{T}}). \tag{29c}$$

They account for the bending deformation of the piezoelectric layers and the so-called full electromechanical coupling, by including the stiffness contribution due to the induced electric potential. Very often the influence of the induced electric potential is neglected and the bending stiffness is further approximated by

$$k_{Mw}^{(\mathrm{NS1})} = Y^{\mathrm{E}}a_1\left(\frac{h_1(h_1+h_2)^2}{2}+\frac{h_1^3}{6}\right) + Y\frac{a_2 h_2^3}{12}, \tag{30}$$

or even by

$$k_{Mw}^{(\mathrm{NS2})} = Y^{\mathrm{E}}\frac{a_1 h_1 h_2^2}{2} + Y\frac{a_2 h_2^3}{12} \tag{31}$$

for very thin piezoelectric layers for which only the membranal behavior is accounted for.

The constitutive coefficients $k_{Mw}^{(\mathrm{NS1})}$ and $e_{MV}^{(\mathrm{NS})}$ are those given by Crawley and Anderson [7] in their Euler–Bernoulli model. The opportunity of correcting the flexural stiffness with the expression (29a) which includes the influence of the induced electric potential is discussed in details in [10,13,15]. Complete electromechanical constitutive equations are provided by Smits et al. [19], Park and Moon [22], and Wang and Cross [21] in their works on cantilevered sandwich and bimorph benders. It can be easily shown that their constitutive coefficients correspond to $k_{Mw}^{(\mathrm{NS1})}$, $e_{MV}^{(\mathrm{NS})}$, and $\varepsilon_{qV}^{(\mathrm{NS})}$.

4.2.2. Null transverse deformation (ND) model

In standard beam modelling, the alternative to the uniaxial stress-state condition (1) is to remove the hypotheses on the transverse stress T_{22} and to assume vanishing transverse deformations S_{22}. The corresponding beam model is obtained by the variational formulation above simply by removing the additional condition on transverse stress (7). In this case we find the following expressions for beam constitutive coefficients (see [30] for further details)

$$k_{Mw}^{(\mathrm{ND})} = \tilde{c}_{11}^{\mathrm{D}}\frac{a_1 h_1^3}{6} + \tilde{c}_{11}^{\mathrm{E}}\frac{h_1(h_1+h_2)^2}{2} + \tilde{c}_{11}\frac{a_2 h_2^3}{12}, \tag{32a}$$

$$e_{MV}^{(\mathrm{ND})} = a_1\tilde{e}_{31}(h_1+h_2), \tag{32b}$$

$$\varepsilon_{qV}^{(\mathrm{ND})} = \frac{2a_1\tilde{\varepsilon}_{33}^{S}}{h_1}. \tag{32c}$$

The null transverse deformation (ND) hypothesis, corresponding to the plane-strain condition, has been used by some authors (see e.g. [11]). In our opinion, it should be also the assumption made in [6,5] to get the electrically induced tip deflection of cantilevered bimorph and sandwich beams (so explaining the high discrepancy they found with respect to the Wang and Cross model [21], which is in plane-stress).

5. Numerical comparisons

In order to validate the present model and show how it enhances standard modelling approaches, some numerical examples are considered. In the following, we analyze how different models estimate the beam constitutive coefficients and how they mimic the 3D distribution of the electromechanical fields. In this context, the results obtained

with numerical finite element simulations on the three dimensional models are taken as reference. The cases of sandwich and bimorph beams with typical cross-sectional aspect ratios are studied in details. The constitutive properties of the piezoelectric and elastic materials considered for the numerical evaluation of expressions (26)–(32) are reported in Table 2. The 3D FE simulations rely on the full constitutive matrices for the piezoelectric material reported in Appendix A. The analysis is based on the Saint-Venant beam assumptions and the consequence of boundary effects are not investigated. For this reason, the numerical simulations on the 3D model are performed in the simple bending conditions, with a suitable distribution of the mechanical loads on the beam bases (see Fig. 3).

5.1. FEM 3D

In order to validate the proposed modelling approach, FEM numerical simulations on 3D models of piezoelectric beams are performed. In particular, the coefficients appearing in the constitutive Eq. (25) are identified by numerical simulations on a simply-supported sandwich beam in uniform bending (see Fig. 3). To this end we consider two different loading conditions for the 3D model:

1. *Moment loading* ($M = \overline{M}$, $V = 0$). By setting to zero the electric voltage V, a through-the-thickness linear pressure distribution having null force resultant and moment resultant $\overline{M}$ is imposed on the beam bases.
2. *Voltage loading* ($M = 0$, $V = \overline{V}$). By setting to zero the pressure on the beam bases, a voltage difference $\overline{V}$ is applied at the electric terminals of the beam.

Table 2
Numerical values of the 3D constitutive coefficients required by the present model for aluminum and the PZT-5H

Elastic layers	
$Y = 1/s_{11} = 69 \times 10^9$ N/m^2	$v = -s_{11}/s_{12} = 0.33$
Piezoelectric layers	
$Y^{\mathrm{E}} = 1/s^{\mathrm{E}}_{11} = 62 \times 10^9$ N/m^2	$v^{\mathrm{E}} = -s^{\mathrm{E}}_{11}/s^{\mathrm{E}}_{12} = 0.31$
$d_{31} = -320 \times 10^{-12}$ m/V	$\beta^{\mathrm{T}}_{33} = 1/\varepsilon^{\mathrm{T}}_{33} = 2.97 \times 10^7$ m/F

Complete expressions for the piezoelectric constitutive matrices, used for 3D finite elements simulations, are given in Appendix A.

If equivalent loadings are applied to the beam model characterized by Eqs. (13) and (25), the axis deflection w_0 at the midspan point and the electric charge Q at the electric terminals are related to the applied moment $\overline{M}$ and voltage $\overline{V}$ by:

$$w_0(\overline{M},\overline{V}) = -\frac{l^2}{8k_{Mw}}\overline{M} - \frac{l^2 e_{MV}}{8k_{Mw}}\overline{V},$$
$$Q(\overline{M},\overline{V}) = \frac{l e_{MV}}{k_{Mw}}\overline{M} - l\left(\varepsilon_{qV} + \frac{e^2_{MV}}{k_{Mw}}\right)\overline{V}.$$

Hence, the following expressions for the beam constitutive coefficients are found:

$$k_{Mw} = -\frac{l^2}{8}\frac{\overline{M}}{w_0(\overline{M},0)}, \tag{33a}$$
$$e_{MV} = -\frac{l}{8}\frac{Q(\overline{M},0)}{w_0(\overline{M},0)} = \frac{w_0(0,\overline{V})}{w_0(\overline{M},0)}\frac{\overline{M}}{\overline{V}}, \tag{33b}$$
$$\varepsilon_{qV} = -\frac{Q^2(\overline{M},0)}{8w_0(\overline{M},0)}\frac{1}{\overline{M}} - \frac{Q(0,\overline{V})}{l}\frac{1}{\overline{V}}. \tag{33c}$$

These formulas are used to identify the beam constitutive coefficients k_{Mw}, e_{MV}, ε_{qV} from the 3D finite element simulations, by detecting w_0 and Q for the two loading conditions above.

The numerical simulations are performed by using the commercial code Ansys 8.0, which contains several 3D and 2D finite elements with piezoelectric capabilities. The 3D coupled-field solid element SOLID5 with piezoelectric option, is adopted. The element has 8 nodes and 4 d.o.f. per node (the three components of the mechanical displacement and the electric potential). A mapped mesh is chosen and the elements are forced to be brick-shaped. For each numerical simulation, the element dimensions are adjusted to get the desired accuracy level, after refinement essays. In particular, the element thickness is set to have at least 4–5

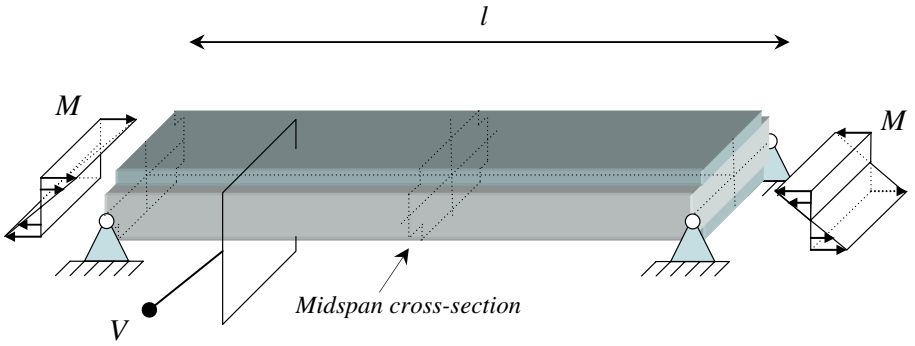

Fig. 3. Simply supported piezoelectric beam in simple bending. For 3D FEM numerical simulations, two different loading conditions are considered: (i) applied electric potential V; (ii) a pair of applied bending moment M at the hinges. In the latter case the bending moments are applied as through-the-thickness linear pressure distribution on the beam bases, in order to approximate an ideal uniform-bending test.

elements along the thickness of each layer;[4] the element length is determined to limit the maximum element aspect ratio to 10–15, which is shown to give accurate results for the considered loading conditions. Typically, the total number of used elements is about 5000–10,000, depending on the cross-sectional geometry. In the FEM model, the different layers are supposed to be perfectly bonded, by constraining corresponding displacements at the interface. The electrodes of the piezoelectric layers are modelled by assigning a single electric degree of freedom (the electrode potential) at all the nodes on the corresponding surface; the corresponding mechanical properties are neglected. The bending moments on the beam bases are applied by imposing an equivalent through-the-thickness linear distribution of surface pressure (see also Fig. 3). This choice is aimed at reducing the boundary effects and to get a better approximation of an ideal uniform-bending test.

5.2. Constitutive coefficients

In Figs. 4 and 5, considering sandwich and bimorph benders, the coefficients appearing in the bending-electric constitutive Eq. (25) are plotted as a function of the thickness ratio between the elastic and the piezoelectric layers. The plots report the estimates given by the different models for the bending stiffness k_{Mw}, the coupling coefficient e_{MV}, and the electric capacitance per unit line ε_{qV}, as appearing in Eq. (25).

In Fig. 4, for a fixed value of the thickness of the elastic layer, the thickness of the piezoelectric layers is varied for $\tau = h_1/h_2$ going from 0 to 1, when assuming $a_1 = 10$ mm, $a_2 = 12$ mm, $h_2 = 2$ mm (see Fig. 2). In Fig. 5, for a fixed thickness of the piezoelectric layers, the thickness of the elastic layer is varied for $\eta = 1/\tau = h_2/h_1$ going from 0 to 1, with $a_1 = a_2 = 10$ mm, $h_1 = 0.5$ mm. Finite element results are obtained through expressions (33) for a beam of length $l = 100$ mm. By analyzing these plots, the following comments can be drawn:

- The values given by the present model are in excellent agreement with the FE results. In particular, they correctly follow the dependence of the equivalent electric capacitance on the thickness ratio between different layers.
- For thin piezoelectric layers ($\tau < 0.1$), the simplified constitutive coefficients given in Equations (27) are in good agreement with FE results. They were obtained as linear approximation (first order Taylor expansions in τ) of the full expressions (26) and they provide handy formulas which can be useful for applications, where the piezoelectric layers are often very thin with respect to the elastic core.
- When using standard modelling approaches, major errors are revealed for the equivalent electric capacitance per unit line ε_{qV}. The models with null transverse stresses (NS) and the model with null transverse deformations (ND) expect two different values, given by Eqs. (29c) and (32c). Both of them are independent of the thickness ratio between the different layers. The FE results show that the actual capacitance, being always comprised between these two values, can significantly differ from both.[5] These errors are explained by keeping in mind that the equivalent capacitance of a piezoelectric sheet depends on the conditions on mechanical stresses and strains. The standard models associate to piezoelectric layers either the value obtained under the condition of null transverse strain or null transverse stress. The actual capacitance corresponds to a more complex stress and strain distribution and differs from both. In particular, like the distribution of transverse strains and stresses, it depends on the cross sectional geometry.
- The ND model remarkably overestimates the bending stiffness and the coupling coefficient. It correctly predicts the piezoelectric capacitance only for very thin piezoelectric layers.
- For thin piezoelectric layers, the NS model gives good estimates of the mechanical stiffness and of the coupling coefficients. However, it introduces appreciable errors also on these quantities when thin and moderately thin elastic layers are considered.
- As previously observed, the errors on the bending stiffness introduced when discarding the influence of the induced potential (expression (30)), are negligible for thin piezoelectric layers. On the other hand, although for thin and moderately thin elastic layers, the errors with respect to FE results become important, they are of the same order of magnitude of those implied by neglecting the influence of transverse stresses.

A special attention must be deserved to the case of the two-layer bending bimorph obtained when $h_2 \to 0$, for which the values given by Smits et al. in [19] are usually taken as reference. The corresponding constitutive coefficients for a particular numerical example are reported in Table 3; the values calculated as in Smits et al. [19] (which correspond to those of NS model neglecting the influence of the induced potential) are also marked by a star in Fig. 5. The comparisons with the 3D FE results shows that only the present model gives accurate estimates. For piezoelectric bimorphs, the models assuming null transverse stresses, which are usually accepted in technical literature, not only miss the value of the piezoelectric capacitance, but imply substantial errors also on the bending stiffness

[4] This condition must be satisfied in order to fit, with the adopted 8-node elements, the actual through-the-thickness distributions of the electromechanical fields (e.g. quadratic electric potential).

[5] For thin piezoelectric layers the capacitance per unit length and per unit thickness ε_{qV}/h_1 is considered, so eliminating the singularity of ε_{qV} for $\tau \to 0$.

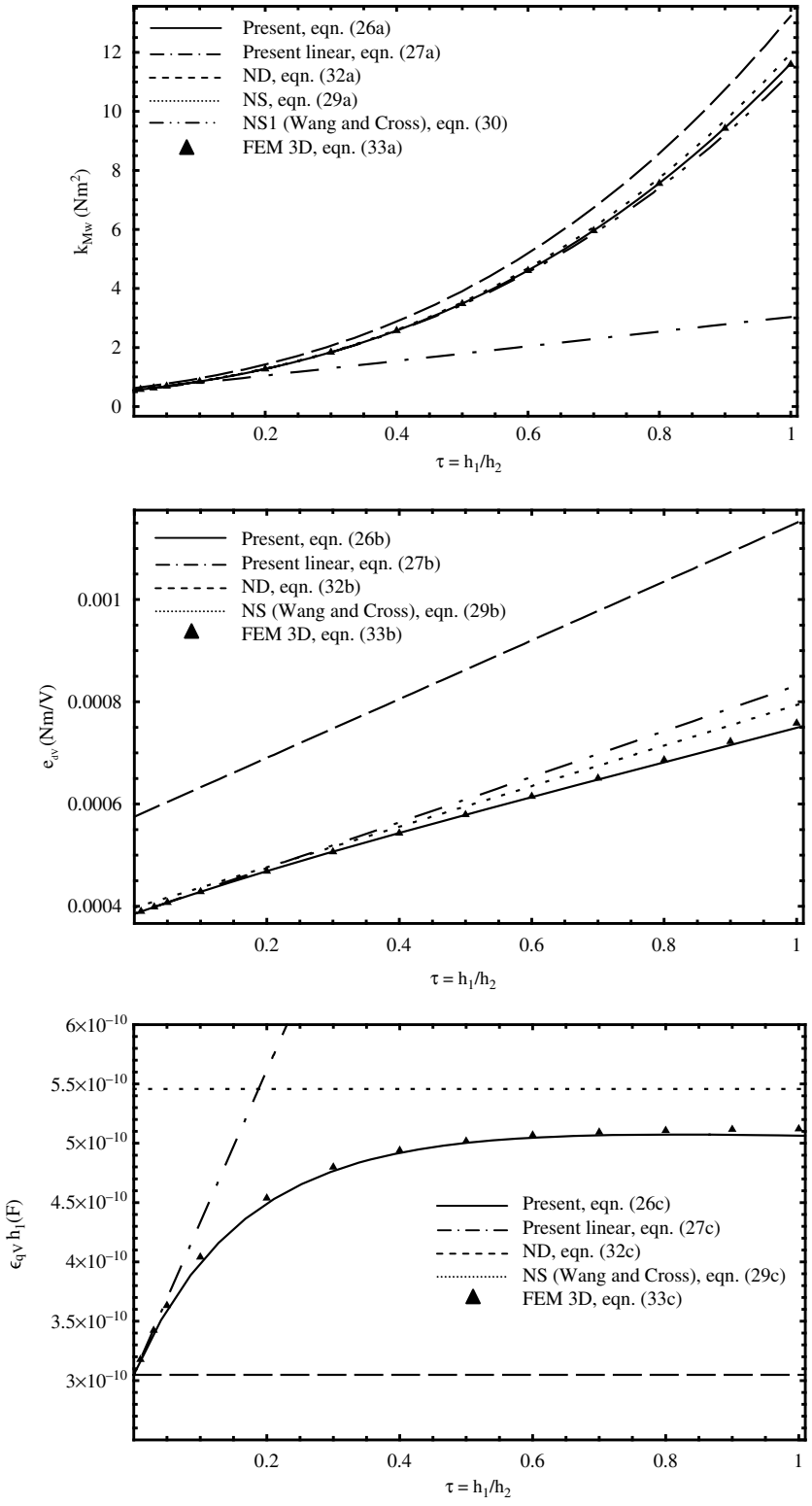

Fig. 4. Electromechanical constitutive coefficients for thin piezoelectric layers as a function of the thickness ratio between piezoelectric and elastic layers $\tau = h_1/h_2$ for $h_2 = 2$ mm, $a_2 = 12$ mm, $a_1 = 10$ mm. Legend: (—) present model, complete expressions (26); (- · -) present model, approximations for thin piezoelectric layers (27); (· · ·) model with null transverse stress (29); (- - -) model with null transverse deformations (32); (- · · -) model with null transverse stress neglecting the induced potential (30), (▲) 3D finite elements.

and the coupling coefficient, even if the influence of the induced potential is taken into account.

In several papers, different models are compared by analyzing the structural deformations and displacements

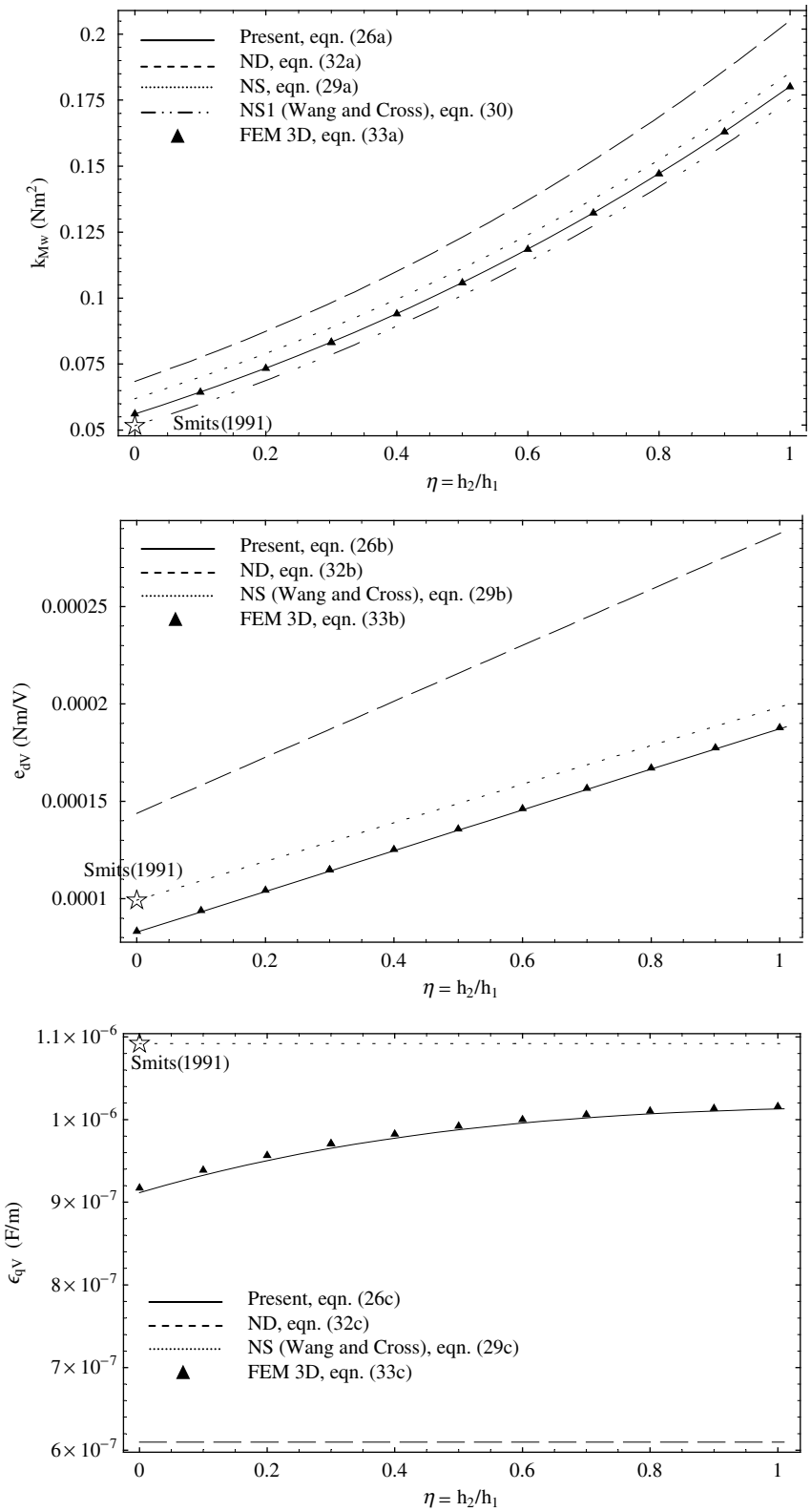

Fig. 5. Electromechanical constitutive coefficients for thin central elastic layer as a function of the thickness ratio between piezoelectric and elastic layers $\eta = h_2/h_1$ for $h_1 = 0.5$ mm, $a_1 = a_2 = 10$ mm. Legend: (—) present model, complete expressions (26); (- · -) present model, approximations for thin piezoelectric layers (27); (· · ·) model with null transverse stress (29); (- - -) model with null transverse deformations (32); (- · · -) model with null transverse stress neglecting the induced potential (30), (▲) 3D finite elements.

induced by an applied electric potential (actuator effect), and the voltage difference induced by a given mechanical deformation under the open-circuit condition (strain sensor effect). We report similar comparisons in Tables 4

Table 3
Electromechanical constitutive coefficients for a two layer bimorph with $a_1 = a_2 = 10$ mm, $h_1 = 0.5$ mm

	Stiffness (N m^2)	Coupling coefficient (N m/V)	Capacitance (μF/m)
FEM 3D	56.11×10^{-3}	83.33×10^{-6}	0.9171
Present k_{Mw}, e_{MV}, ε_{qV}	56.16×10^{-3}(+0.08%)	82.83×10^{-6}(−0.60%)	0.9116(−0.60%)
Standard NS–NS1 $k_{Mw}^{(NS)}$, $e_{MV}^{(NS)}$, $\varepsilon_{qV}^{(NS)}$	61.89×10^{-3} (+10.3%)	99.20×10^{-6}(+19.0%)	1.0918(+19.05%)
$k_{Mw}^{(NS1)}$	51.67×10^{-3}(−7.93%)		
Standard ND $k_{Mw}^{(ND)}$, $e_{MV}^{(ND)}$, $\varepsilon_{qV}^{(ND)}$	68.46×10^{-3}(+22.0%)	143.8×10^{-6}(+72.5%)	0.6097(−33.52%)

Comparison between the values given by the present model, the ND model, the NS model, and the NS model neglecting the influence of the induced potential (NS1). The coefficients found by finite elements numerical simulations on the 3D model are taken as reference and the corresponding relative errors are reported in parenthesis.

Table 4
Bending curvature per unit voltage (e_{MV}/k_{MV}) at null bending moment condition for a two-layer bimorph with $a_1 = a_2 = 10$ mm, $h_1 = 0.5$ mm

	$w''/V\|_{M_1=0}$ (m^{-1} V^{-1})	Error (%)
FEM 3D ($8w_0(0,1)/l^2$)	1.485×10^{-3}	
Present (e_{MV}/k_{MV})	1.475×10^{-3}	−0.68058
Standard NS ($e_{MV}^{(NS)}/k_{MV}^{(NS)}$)	1.603×10^{-3}	7.95425
Standard NS1 ($e_{MV}^{(NS)}/k_{MV}^{(NS1)}$)	1.920×10^{-3}	29.2958
Standard ND ($e_{MV}^{(ND)}/k_{MV}^{(ND)}$)	2.100×10^{-3}	41.4201

Comparison between the present model, the ND model, the NS model, the NS model without the influence of the induced potential (NS1) and the 3D FEM result. The latter is found from the uniform bending test in Fig. 3 with $l = 100$ mm.

Table 5
Induced voltage per unit curvature at null electric charge ($-V/w'|_{q=0} = e_{MV}/\varepsilon_{qV}$) for a two-layer bimorph with $a_1 = a_2 = 10$ mm, $h_1 = 0.5$ mm

	$-V/w''\|_{q=0}$ (m V)	Error (%)
FEM 3D	90.8625	
Present (e_{MV}/ε_{qV})	90.8622	−0.0003
Standard NS and NS1 ($e_{MV}^{(NS)}/\varepsilon_{qV}^{(NS)}$)	90.8591	−0.0037
Standard ND ($e_{MV}^{(ND)}/\varepsilon_{qV}^{(ND)}$)	235.85	+159.57

Comparison between the present model, the ND model, the NS model, the NS model without the influence of the induced potential (NS1) and the 3D FEM result. The latter are obtained on a beam of length $l = 100$ mm in uniform bending and open circuit condition.

and 5. Table 4 details the different estimates found for the curvature induced by an unit voltage in a two-layer bimorph where the bending moment M_1 is null. Table 5 compares those for the electric voltage induced by a given curvature w'' for a beam in uniform bending under the open-circuit condition.[6] The analysis of these results, besides confirming the performance of the present modelling approach, can also partially explain why the substantial errors shown in Table 3 for the model with null transverse stress have not been revealed in experimental and numerical works. Table 4 shows that the curvature induced by an applied potential difference is proportional to the ratio between the coupling and the stiffness coefficients. The NS model which overestimates both the coupling and the stiffness, implies only a minor error[7] on their ratio. On the other hand, the version of the NS model which neglects the induced potential (NS1), while keeping the same coupling coefficient, underestimates the bending stiffness and induces much more evident errors in their ratio. In Table 5, the cancellation-of-errors effect in the NS model is even more evident: the estimates for the electric potential induced by a given curvature found by the proposed model, the NS model, and FE almost coincide. Table 5 shows also that the quadratic contribution of the electric potential does not have any direct influence on strain sensing, since the mechanical stiffness does not play any role in this case. On the other hand, neglecting the quadratic potential leads to a not correct prediction of the deformation induced by applied mechanical forces and, indirectly, of the force sensing effect. In our opinion, Tables 3–5 can help distinguishing between errors due to plane-strain and plane-stress hypotheses and the neglect of the induced potential, as attempted in [26].

5.3. Field distribution

A deeper understanding of the features of the proposed model and of the limits of standard modelling approaches can be got by analyzing how they simulate the 3D distributions of the electromechanical fields. Also in this case, the 3D finite element solutions are taken as reference.

[6] The uniform bending hypothesis allows for assuming that the charge per unit line q is constant along the beam axis and that the open circuit condition (null total charge Q) directly implies that charge per unit line is null. So that the induced voltage is calculated by (25) as. $V/w'|_{q=0} = -e_{MV}/\varepsilon_{qV}$.

[7] Although being still around 8%, it can be confused with the accuracy of the experimental data and/or influence of other non-modelled effects, as non-perfect bonding.

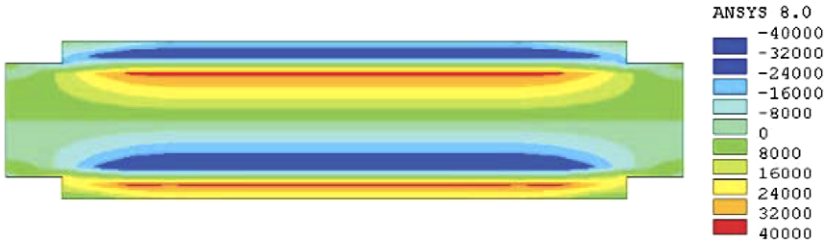

Fig. 6. Contour plot of the 3D FEM results for the transverse stress T_{22} on the midspan cross section of the simply supported beam in Fig. 3 for applied unit voltage and null bending moment ($V = 1$ V, $M = 0$). Numerical values in N/m^2.

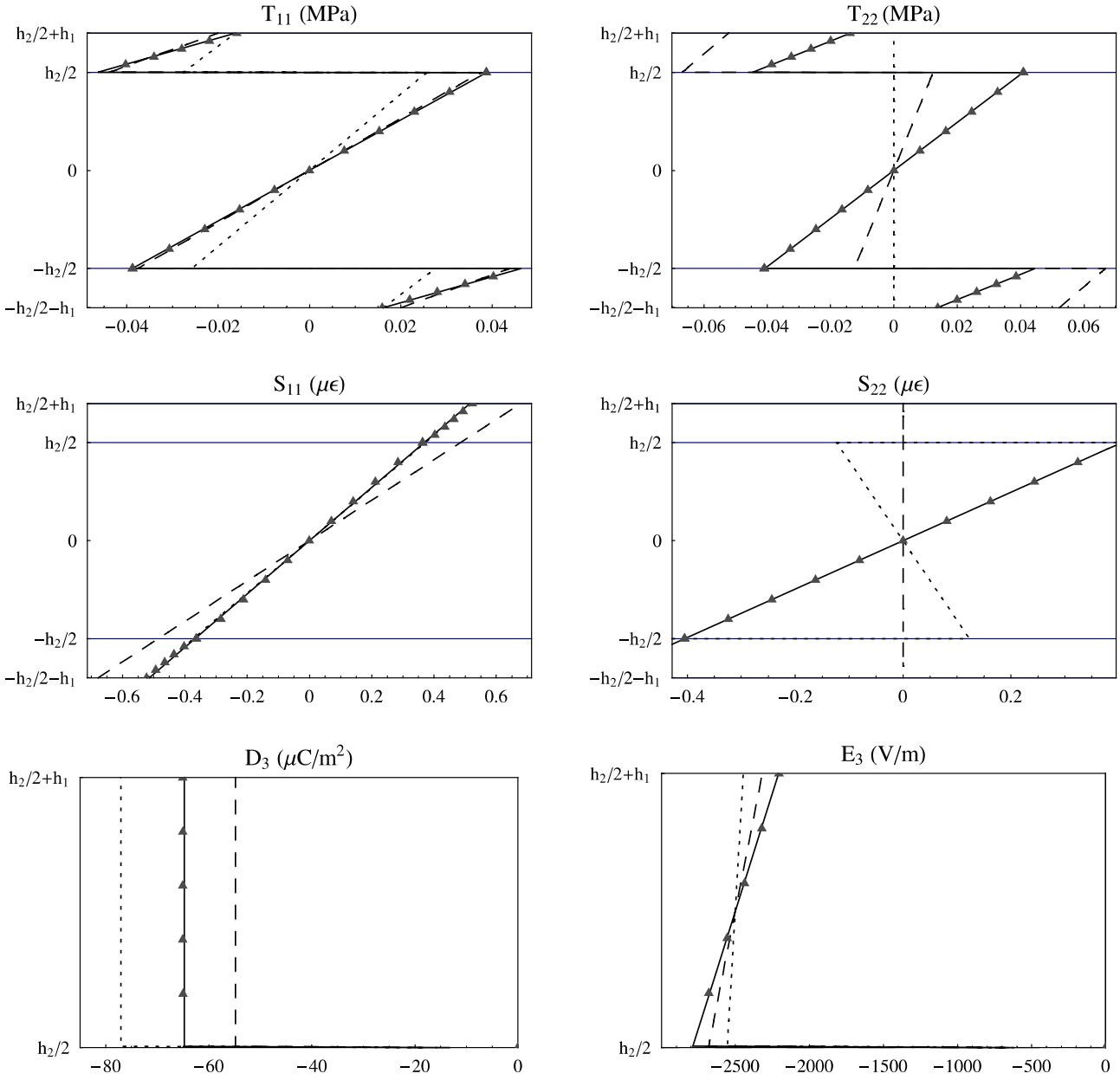

Fig. 7. Through-the-thickness distribution of the electromechanical fields for applied unit voltage and null bending moment for the piezoelectric sandwich beam in Fig. 3 ($V = 1$ V, $M = 0$): axial and transverse (width direction) normal stresses T_{11} and T_{22}, axial and transverse deformations S_{11} and S_{22}, electric displacement D_3 and electric field E_3 along the layers thickness. Legend: (—) present model; (···) model with null transverse stress; (--,) model with null transverse deformations; (▲) 3D finite elements. The distributions are taken at the central z-line of the midspan cross-section of the beam in Figs. 2 and 3, where $h_2 = 2$ mm, $a_2 = 12$ mm, $h_1 = 0.4$ mm, $a_1 = 10$ mm. For FE numerical simulations, the beam length equals $l = 100$ mm.

A typical contour plot of the distribution of the transverse stress T_{22} obtained with the 3D finite elements is reported in Fig. 6. It is taken at the midspan cross-section of the simply-supported sandwich beam in Fig. 3, under the loading condition $V = 1$ V, $M = 0$. It clearly shows that, for imposed electric potential, important transverse stresses are induced in the three-layer region. These stresses vanish in the single-layer regions, with an edge effect around the ends of the piezoelectric layers.

In the proposed mixed model, the calculation of the field distributions used for the evaluation of the internal energy requires to find: (i) the mechanical displacement fields $u(x)$ and $w(x)$ and the electric potential V solving equations (13)–(14) and (24) for the given loading and boundary conditions; (ii) the corresponding transverse deformations by Eq. (19). Hence, the distribution of the mechanical stress and electric displacement is obtained through Eqs. (16) and (6). The associated distributions of the strain and the electric potential are found by the 3D constitutive equations.

The plots in Figs. 7–10 compare the through-thickness field distributions obtained with the proposed model to those associated to the 3D finite elements, the NS model, and the ND model. The distributions are taken at the cen-

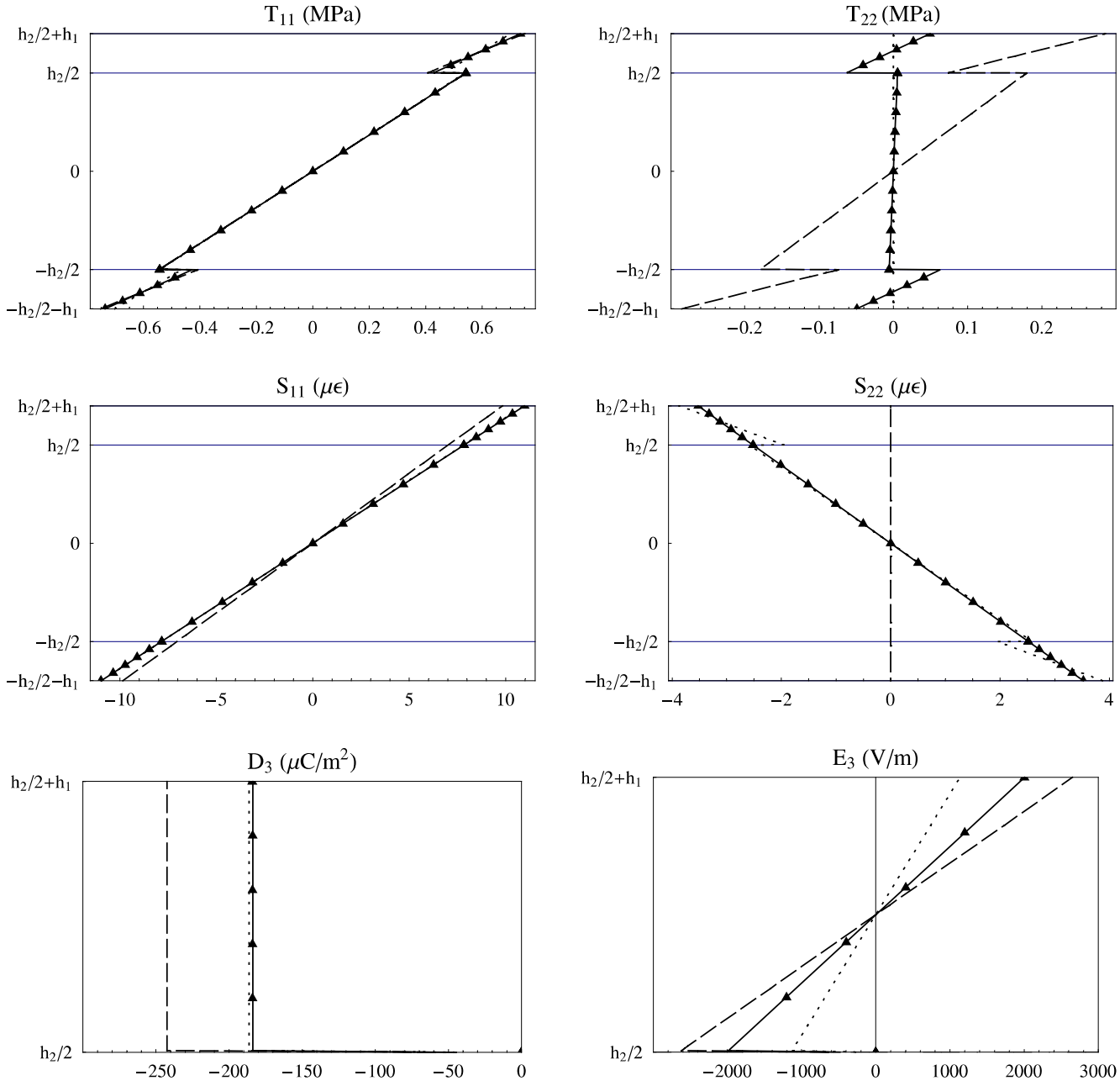

Fig. 8. Through-the-thickness distribution of the electromechanical fields for applied bending moment and null electric voltage for the piezoelectric sandwich beam in Fig. 3 ($M = 0.01$ N m, $V = 0$). For testing geometry and plot legend refer to Fig. 7.

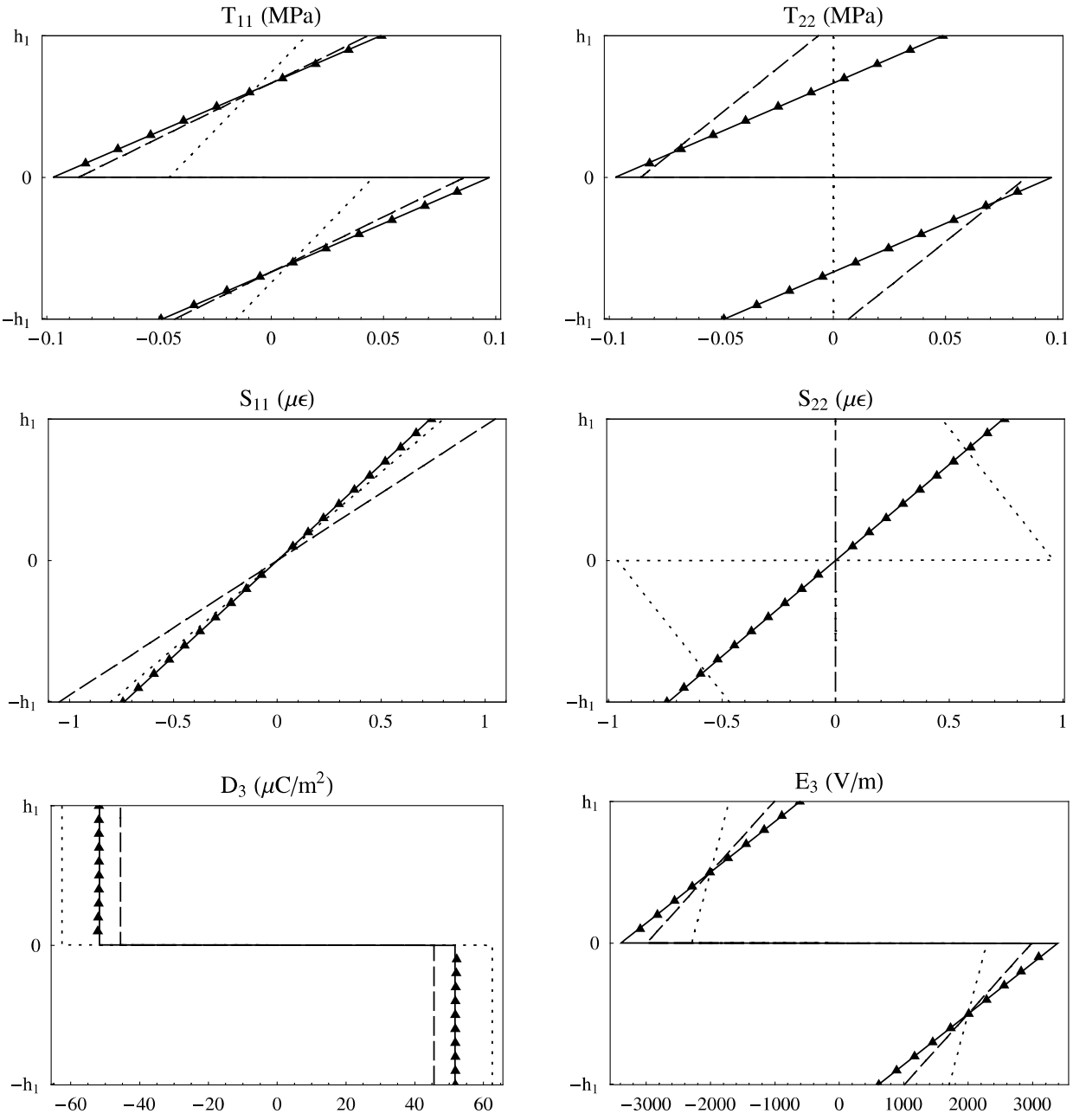

Fig. 9. Through-the-thickness distribution of the electromechanical fields for applied unit voltage and null bending moment ($V = 1$ V, $M = 0$) for a two-layer bimorph piezoelectric beam (layer arrangement as in Fig. 2 with $h_2 = 0$). The distributions are taken at the central z-line of the midspan cross-section of the beam in Figs. 2 and 3, where $h_1 = 0.5$ mm, $a_1 = 10$ mm, $h_2 = 0$. For FE numerical simulations, the beam length equals $l = 100$ mm. For the plot legend refer to Fig. 7.

tral *z-line* of the midspan cross-section of the sandwich beam. Referring to the boundary conditions and notation introduced in Fig. 3, two different loading conditions are considered, both for the sandwich (Figs. 7 and 8) and bimorph (Figs. 9 and 10) beams: (i) applied electric potential with null bending moment; (ii) applied bending moment with short-circuited electrodes. The analysis of the field distributions confirms the ability of the proposed model to correctly mimic the 3D one. It clearly shows that, for imposed electric potential, *axial and transverse stresses are of the same order of magnitude*.[8] Hence, it can be stated that *the uniaxial-stress hypothesis is not physically grounded*

[8] The hypothesis of vanishing transverse stress resultants in the form (7) allows also for correctly predicting that the transverse stresses vanish pointwise in the cross-sectional regions where a single elastic layer is present. This is an improvement with respect to the model presented by the authors in [30]. The edge effects are still completely neglected and the modification of the stress distribution between the single-layer and the three-layers region is abrupt.

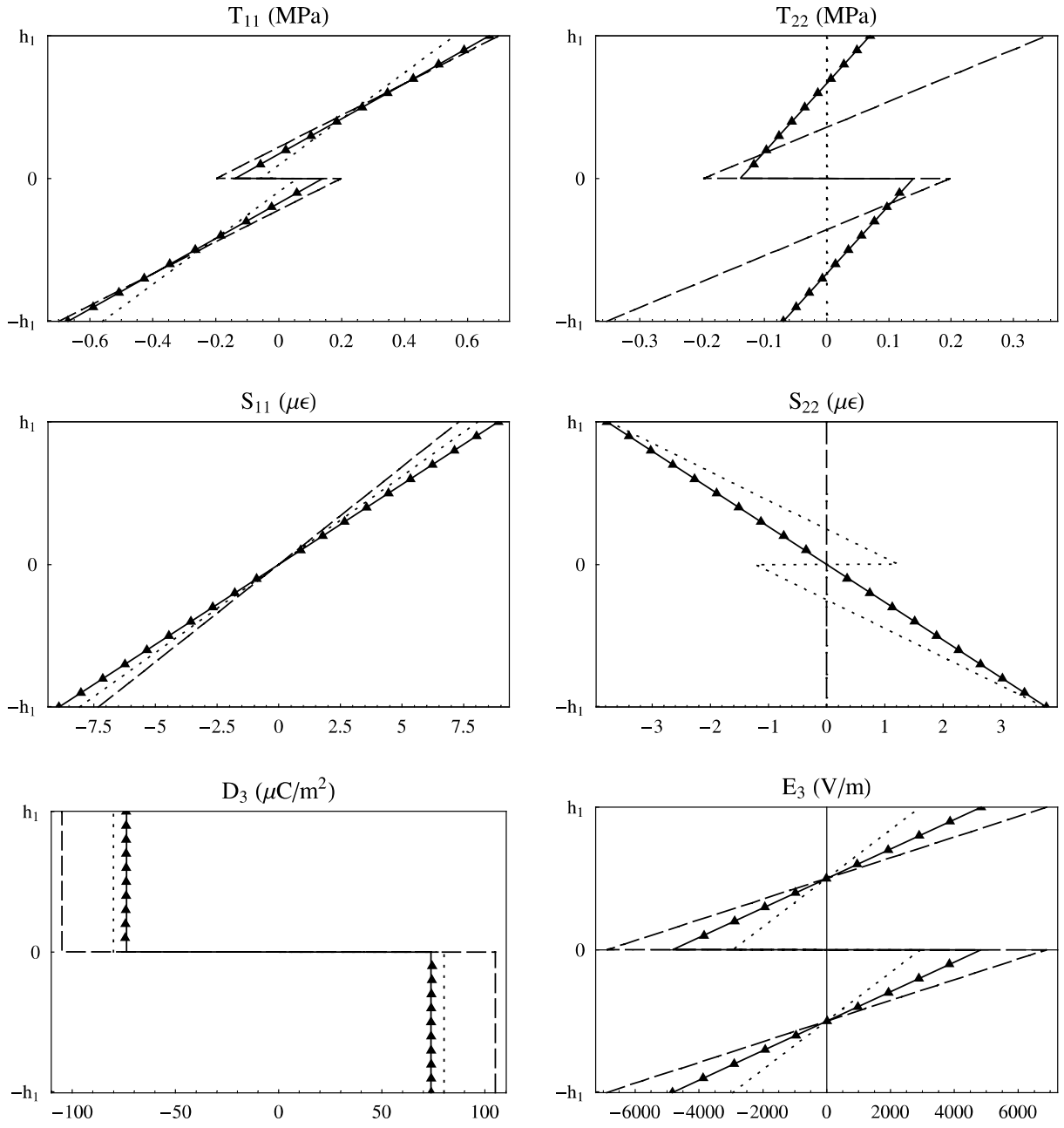

Fig. 10. Through-the-thickness distribution of the electromechanical fields for applied unit bending moment and null electric voltage for a two-layer bimorph piezoelectric beam ($M = 0.001$ N m, $V = 0$, layer arrangement as in Fig. 2 with $h_2 = 0$). For testing geometry, refer to Fig. 9, for plot legend to Fig. 7.

in this case. The NS model, by assuming null transverse stress, neglects completely transverse interactions between different layers. In particular, although different layers are assumed to be perfectly bonded, the NS model let them free to slide one on each other along the beam width. On the other hand, in the ND model the transverse stresses arising in the piezoelectric layers when an electric potential is applied, are not correctly transmitted to the elastic one (dashed line for the distribution of T_{22}). In piezoelectric beams, blocking Poisson-like transverse strains, in addition to a well known stiffening phenomenon, leads also to an overestimate of the axial-electric electromechanical coupling (see e_{MV} plots in Figs. 4 and 5). This effect is caused by ignoring the elastic energy stored in the transverse deformations. Moreover, the errors in the distributions of the mechanical deformations and stresses influence also the accuracy on the electrical fields. Indeed, by piezoelectric coupling, they indirectly induce errors in the electric displacement and in the linear contribution to the electric field (see the plots for D_3 and E_3). This is the reason why the electric capacitance per unit line is misestimated by the NS and ND models.

The phenomena underlined above are still more important for the two-layers bending bimorphs, whose field dis-

tributions for applied bending moment and electric potential are reported in Figs. 9 and 10. They show that, differing from what found for sandwich beams with thin piezoelectrics, the amplitude of transverse stresses is comparable to that of axial ones also for applied bending moment and null electric potential. Moreover, the transverse stresses are of the same order of magnitude throughout the beam thickness. The NS model, by neglecting these contributions, introduces remarkable inaccuracies in the estimate of the elastically stored energy, so leading to the errors in the bending stiffness and in the coupling coefficients reported in Table 3.

6. Conclusions

In the present paper, beam models of piezoelectric laminates accounting for two-fold electromechanical coupling were discussed. We noted that some hypotheses on the stress and strain distributions, although widely accepted in the technical literature, are not physically grounded. In particular, finite element numerical simulations on 3D models show that, in piezoelectric laminates, the normal transverse stresses and strains (transverse meaning width direction) are not negligible. Hence, neither the plane-stress nor the plane-strain assumptions are acceptable. We use a mixed variational formulation to establish a beam model where the effects of transverse stresses and strains are taken into account. In the proposed model, the transverse stresses are supposed to be layerwise linear. They are determined through integral conditions (null through-the-thickness force and moment resultants), which are imposed in the variational formulation through the Lagrange multiplier method. Moreover, the mixed approach allows us to straightforwardly include the effect of the so called induced potential without adding redundant electric degrees-of-freedom. As a main advantage of the proposed formulation, the beam governing equations in the final form fit into the format of a standard electromechanical Euler–Bernoulli model with a single electric degree of freedom. The effects of the transverse stresses and strains and of the quadratic contribution to the electric potential are accounted for in the beam constitutive coefficients, which are suitably corrected. For sandwich and bimorph benders, simple analytical expressions of the corrected electromechanical constitutive coefficients were provided. Their evaluation requires the knowledge of few material properties and they can be promptly used in applications to replace standard formulas.

The model was validated through comparisons with standard modelling approaches and results from 3D finite element numerical simulations in simple bending. A detailed discussion on the influence and the plausibility of possible assumptions in beam modelling of piezoelectric laminates was carried out and a deeper understanding of the main phenomena is achieved. Focusing on sandwich and bimorph benders, the comparisons were made in terms of the estimates of the electromechanical beam constitutive coefficients and the associated through-the-thickness distributions of the three-dimensional fields. The analysis led to the following conclusions:

1. The proposed model accurately predicts all the relevant electromechanical constitutive parameters and correctly follows the field distributions found by 3D finite element analysis, independently of the thickness ratio between piezoelectric and elastic layers.
2. For piezoelectric sandwiches and bimorphs, the standard models fail to predict the equivalent piezoelectric capacitance.
3. For piezoelectric sandwiches with thin elastic layers and for bimorph benders, the standard models introduce appreciable errors not only on the piezoelectric capacitance, but also on the bending stiffness and the coupling coefficient.
4. If transverse stresses are neglected, including the effect of quadratic contribution to the electric potential does not improve the accuracy on the estimate of the mechanical stiffness (see Table 3). It improves the prediction of the actuating and sensing effect only for a cancellation-of-error phenomenon.

To our opinion further developments of the present work can include:

- Analysis of special boundary value problems (e.g. cantilever beam with applied force or bending moment), to assess the validity of the present model in presence of boundary effects.
- Proper introduction of the effect of transverse stresses on beam models more refined than the Euler–Bernoulli one, by revisiting the literature on equivalent single-layer Timoshenko models [15] and layerwise approaches [9] and by accounting also for influence of the bonding layers [27].
- Developing a corrected Euler–Bernoulli finite element for piezoelectric laminates and, after the previous point, also a generation of more accurate beam elements including the effect of transverse stresses.
- Studying the effect of transverse stresses and deformations also in other context as in active constrained layer damping [23] or in layered beams subjected to thermal loads.

Acknowledgements

The present work has been done in the framework of the joint research project ‘‘Smart materials and structures: structural control using distributed piezoelectric transducers and passive electric networks’’ funded by the international agreement between CNRS (France) and CNR (Italy), project no. 16283.

Appendix A. Piezoelectric constitutive matrices

Considering the 3D piezoelectric constitutive equations in the $T-E$ form and standard Voigt notation [31] ($i,j=1,\dots,6$; $h,k=1,2,3$)

$$S_i = s^{\mathrm{E}}_{ij} T_j + d_{ik} E_k$$
$$D_h = d_{jh} T_j + \varepsilon^{\mathrm{T}}_{hk} E_k$$

the following numerical values for the constitutive matrices are assumed:

$$[s^{\mathrm{E}}] = \begin{bmatrix} 16.13 & -5.0 & -8.164 & 0 & 0 & 0 \\ -5.0 & 16.13 & -8.164 & 0 & 0 & 0 \\ -8.164 & -8.1642 & 20.0 & 0 & 0 & 0 \\ 0 & 0 & 0 & 42.52 & 0 & 0 \\ 0 & 0 & 0 & 0 & 42.52 & 0 \\ 0 & 0 & 0 & 0 & 0 & 42.26 \end{bmatrix} \times 10^{-12} \frac{\mathrm{m}^2}{\mathrm{N}}$$

$$[d] = \begin{bmatrix} 0 & 0 & 0 & 0 & 865.4 & 0 \\ 0 & 0 & 0 & 865.4 & 0 & 0 \\ -320.0 & -320.0 & 650.0 & 0 & 0 & 0 \end{bmatrix} \times 10^{-12} \frac{\mathrm{m}}{\mathrm{V}}$$

$$[\varepsilon^{\mathrm{T}}] = \begin{bmatrix} 30.97 & 0 & 0 \\ 0 & 30.97 & 0 \\ 0 & 0 & 33.64 \end{bmatrix} \times 10^{-9} \frac{\mathrm{C}}{\mathrm{V\,m}}$$

These values are used for the finite element simulations on the 3D model and contain also those given in Table 2, which are the only ones required for the presented beam model. They refer to the material properties of PZT-5H and are extracted from the datasheets provided by *Piezo System, Inc*. (see www.piezo.com).

References

[1] Chopra I. Review of state of art of smart structures and integrated systems. AIAA J 2002;40:2145–87.

[2] Saravanos DA, Heylinger PR. Mechanics and computational models for laminated piezoelectric beams, plates, and shells. Appl Mech Rev 1999;52:305–20.

[3] Gopinathan SV, Varadan VV, Varadan VK. A review and scritique of theories for piezoelectric laminates. Smart Mater Struct 2000;9:24–48.

[4] Vel SS, Batra RC. Three-dimensional analytical solution for hybrid multilayered piezoelectric plates. J Appl Mech 2000;67(3):558–67.

[5] He LH. Three-dimensional analysis of some symmetric hybrid piezoelectric laminates. Z Angew Math Mech 2000;80(5):307–18.

[6] Lim CW, He LH. Three-dimensional exact solutions for the electromechanical response of triple layer piezoelectric actuators. Smart Mater Struct 2004;13:1050–8.

[7] Crawley EF, Anderson EH. Detailed models of piezoceramic actuation in beams. J Intell Mater Syst Struct 1990;1:12–25.

[8] Sirohi J, Chopra I. Fundamental understanding of piezoelectric strain sensors. J Intell Mater Syst Struct 2000;11:246–57.

[9] Kapuria S, Dumir PC, Ahmed A. An efficient coupled layerwise theory for dynamic analysis of piezoelectric composite beams. J Sound Vibr 2003;261:927–44.

[10] Sze KY, Yang XM, Fan H. Electric assumptions for piezoelectric laminate analysis. Int J Solids Struct 2004;41:2363–82.

[11] Kusculuoglu ZK, Fallahi B, Royston TJ. Finite element model of a beam with a piezoceramic patch actuator. J Sound Vibr 2004;276(1–2):27–44.

[12] Costa Branco PJ, Dente JA. On the electromechanics of a piezoelectric transducer using a bimorph cantilever undergoing asymmetric sensing and actuation. Smart Mater Struct 2004;13:631–42.

[13] Benjeddou A. Advances in piezoelectric finite element modeling of adaptive structural elements: a survey. Comput Struct 2000;76:347–63.

[14] Fernandes A, Pouget J. Analytical and numerical approaches to piezoelectric bimorph. Int J Solids Struct 2003;40(17):433.

[15] Krommer M. On the correction of the Bernoulli–Euler beam theory for smart piezoelectric beams. Smart Mater Struct 2001;10:668–80.

[16] Hagood NW, von Flotow A. Damping of structural vibrations with piezoelectric materials and passive electrical networks. J Sound Vibr 1991;146(2):243–68.

[17] dell'Isola F, Maurini C, Porfiri M. Passive damping of beam vibrations through distributed electric networks and piezoelectric transducers: prototype design and experimental validation. Smart Mater Struct 2004;13(2):299–308.

[18] Andreaus U, dell'Isola, Porfiri M. Piezoelectric passive distributed controllers for beam flexural vibrations. J Vibr Control 2004;10(5):625–59.

[19] Smits JG, Dalke SI, Cooney TK. The constitutive equations of piezoelectric bimorphs. Sensors Actuat A 1991;28:41–61.

[20] Lu P, Lee KH. An alternative derivation of dynamic admittance matrix of piezoelectric cantilever bimorph. J Sound Vibr 2003;266:723–35.

[21] Wang QM, Cross LE. Constitutive equations of symmetrical striple layer piezoelectric benders. IEEE Trans Ultrason Ferroelectrics Freq Control 1999;46(6):1343–51.

[22] Park JK, Moon WK. Constitutive relations for piezoelectric benders under various boundary conditions. Sensors Actuat A 2005;117:159–67.

[23] Trindade MA, Benjeddou A, Ohayon R. Finite element modelling of hybrid active-passive vibration damping of multilayer piezoelectric sandwich beams—Part I: Formulation. Int J Numer Methods Eng 2001;51:835–54.

[24] Gaudenzi P, Carbonaro R, Benzi E. Control of beam vibrations by means of piezoelectric devices: theory and experiments. Compos Struct 2000;50:373–9.

[25] Park CH. Dynamics modelling of beams with shunted piezoelectric elements. J Sound Vibr 2003;268:115–29.

[26] Poizat C, Benjeddou A. On analytical and numerical modelling of piezoelectric bimorphs. In: Topping, Mota Soares, editors. Proceedings of 7th international conference on computational structures technology, CST 2004 Lisbon, 2004. Session: Modelling and simulation of adaptive beams and bimorphs; Paper no. 7.

[27] Beckert W, Pfundtner G. Analysis of the deformational behaviour of a bimorph configuration with piezoelectric actuation. Smart Mater Struct 2002;11:599–609.

[28] Wang SY. A finite element model for the static and dynamic analysis of a piezoelectric bimorph. Int J Solids Struct 2004;41:4075–96.

[29] Abramovich H, Meyer-Piening HR. Induced vibrations of piezolaminated elastic beams. Compos Struct 1998;43:47–55.

[30] Maurini C, Pouget J, dell'Isola F. On a model of layered piezoelectric beams including transverse stress effect. Int J Solids Struct 2004;41(16–17):4473–502.

[31] Ikeda T. Fundamentals of piezoelectricity. Oxford: Oxford University Press; 1990.

[32] Reissner E. On a certain mixed variational theorem and a proposed application. Int J Numer Methods Eng 1984;20:1366–8.

[33] Washizu K. Variational methods in elasticity and plasticity. Pergamon Press; 1982.

[34] Yang JS, Batra RC. Mixed variational principles in nonlinear piezoelectricity. Int J Nonlinear Mech 1995;30(5):719–26.

[35] Teresi L, Tiero A. On variational approaches to plate models. Meccanica 1997;32:143–56.